



Mohamed Khider University of Biskra

Faculty of Exact Sciences and Nature and Life

Department of Matter Sciences

Master Dissertation

Sciences of Matter

Physique

Energy physics and renewable energies

Réf. :

Submitted by:

Messeddek Roumaissa

Messeddek Loubna

On: June 2021

The effect of solvents on the properties of thin films of (TiO₂) deposited by sol gel (spin-coating).

Board of Examiners :

Marmi Saida	MCA	University of Biskra	Chairperson
Saidi hanane	Pr	University of Biskra	Supervisor
Bennaceur Kheira	MCA	University of Biskra	Examiner

Dedication

In the Name of Allah the Most Merciful

This modest work is dedicated to:

To our dear parents who have always been the major source of inspiration behind all our efforts and achievements. Thank you for always being our best supporters.

To the sweetest brothers ever: Rouchdi and Ali.

To our lovely sisters: Imen, Nesrin and Amel.

To all members Messeddek family.

To our lovely Friends: Nour, Houda, Rihem, Afaf, Tahani, Joumana, Rania and Aicha.

Thank you for your support.

*We are so lucky that all of you are in our life. **THANK YOU.***

Lastly, we'd like to thank ourselves, and give ourselves a big pat on the back.

Twins Loubna & Ruomaissa

Acknowledgements

In the name of Allah the Most Merciful the More Gracious, all thanks to Allah the Lord of the Heavens and Earth and Peace be upon Mohamed and his Companions.

*After that, we would like to offer sincere thanks to our supervisor Mrs. **Saidi Hanan**, for her precious guidance, assistance and support. We also extend our thanks to Prof. **Attaf Abdallah**. His helpful door was always open whenever we ran into a trouble spot or had a question about our research.*

*Special thanks for PhD Student **Benkhetta Okba** who gave us a helping hand during the work and research period .and we thank also all the members of thin films“ laboratory of our university in particular: **D.Nour el houda** ,**M.Radhia** and **B.Yousef**.*

*We would like also to thank the members of the jury , Mrs **Marmi Saida** and Mrs **Bennaceur Kheira** who spend their time to check and evaluate this research study.*

Table of contents

<i>Dedication</i>	i
Acknowledgements	ii
Table of contents	iii
List of Figures	vi
List of Tables	ix
Introduction General	1
Chapter I:Thin Films deposition and characterization techniques	
I.1 Thin film technology	3
I.1.1 This film feature	3
I.1.2 Formation stages of thin films	3
I.1.3 Thin film growth modes	4
I.2 Deposition techniques	5
I.2.1Sol-gel technology	5
I.2.2 Sol-gel method	6
I.2.2.1 Sol-gel chemistry tends to be particularly sensitive to the following parameter	9
I.2.2.1.1 Precursor properties	9
I.2.2.1.2 Reaction temperature	9
I.2.2.1.3 Gel time	9
I.2.2.1.4 Solvent	10
I.2.2.1.5 Properties and concentrations of catalyst	10
I.2.2.1.6 Ratio of water to metal alkoxide	10
I.2.2.2 The relationship between gel time and reaction temperature	11
I.2.2.3 Advantages of sol-gel method	11
I.3 Methods used to apply sol-gel on substrates	12

I.3.1 Spin coating.....	12
I.3.1.1 Description of spin coating process.....	12
I.3.1.2 Thin films characteristics.....	15
I.3.1.3 Advantages disadvantages of Spin Coating.....	16
I.3.2 Drying.....	16
I.3.3 Annealing.....	16
I.4 Thin film characterization.....	16
I.4.1 X-ray diffraction.....	16
I.4.1.1 Determination of the crystallite size.....	18
I.4.1.2 Determination the dislocation density.....	18
I.4.1.3 Determination of the deformation.....	18
I.4.2 Spectroscopy(UV-VISIBLE).....	19
I.4.2.1 The thickness of the film.....	21
I.4.2.2 Optical band gap (E_g).....	22
I.4.2.3 Urbach energy (E_u).....	23
I.4.3 Scanning electron microscopy (SEM).....	24
I.4.4 Four-point probe method.....	26

Chapter II :Generalities about titanium dioxide TiO₂.

II.1 Titanium dioxide.....	28
II.2 Properties of TiO ₂	28
II.2.1 Structural properties.....	28
II.2.1.1 Anatase.....	28
II.2.1.2 Brookite.....	29
II.2.1.3 Rutile.....	30
II.2.1.4 Stability of TiO ₂ phases.....	32
II.2.2 Optical properties.....	33
II.2.3 Electrical properties.....	33

II.2.4 Photocatalytic properties.....	34
II.3 Importance and applications of TiO ₂ thin films.....	35
Chapter III :Experimentalprocedures, results and discussions.	
III.1 Detailed experimental condition.....	38
III.1.1 Used apparatus (Spin coater).....	38
III.1.2 Materials used.....	38
III.1.2.1 Properties of the materials used.....	38
III.1.2.2 Why we used of these alcohol solvents ?.....	41
III.1.3 Preparation of TiO ₂ thin films.....	41
III.1.3.1 Solution preparation.....	41
III.1.3.2 Preparation of the substrate.....	41
III.1.3.3 Depositing of thin films.....	43
III.2 Results and discussions.....	44
III.2.1 Adhesion test.....	44
III.2.1.1 Simple test used.....	44
III.2.2 The thickness of the film.....	44
III.2.3 Structural characterization.....	46
III.2.3.1 Crystallite size.....	48
III.2.3.2 The dislocation density and deformation.....	50
III.2.4 The optical properties.....	51
III.2.4.1 Optical Band gap energy.....	53
III.2.4.2 The Energy of urbach E _u (disorder).....	55
III.2.5 Surface Morphological Study.....	56
III.2.6 Chemical Properties.....	57
III.2.7 Electrical Properties.....	59
General conclusion.....	62
References Introduction and Chaptre I.....	63

References Chapitre II.....	65
References chapter III.....	67

List of Figures

Figure.I.1 Schematics and FE-SEM images of the stages of thin film growth.....	4
Figure.I.2 Schematic diagram of three basic growth modes: (a) Frank-Van DerMerwe, (b) Volmer-Weber(VW), (c) the Stranski-Krastanov(SK)	4
Figure.I.3 Thin films deposition techniques.....	5
Figure.I.4 Stages of the sol-gel process.....	6
Figure.I.5 Sol-gel reactions of organically modified alkoxide precursors (Hydrolysis).....	7
Figure.I.6 Sol-gel reactions of organically modified alkoxide precursors (Condensation)...	8
Figure.I.7 Several types of OH bridges can be formed by olation condensation process.....	8
Figure.I.8 Formation of oxo-bridging links between two metal centers.....	9
Figure.I.9 Technical trends of thin films.....	11
Figure.I.10 Preparation of coatings by sol-gel method	12
Figure.I.11 Four distinct stages to spin coating.....	14
Figure.I.12 Relation between film thickness Vs speed.....	15
Figure.I.13 Principle of Bragg's law	17
Figure.I.14 Schematic of UV- visible spectrophotometer	20
Figure. I.15 Transmittance spectra of TiO ₂ thin films.....	20
Figure.I.16 System of an absorbing thin film on a thick finite transparent substrate.....	21
Figure.I.17 Method of interference fringes to determinate the thickness.....	22

Figure.I.18 Determination of the optical band gap direct (E_g).....	23
Figure.I.19 Determination of the optical band gap indirect (E_g).....	23
Figure.I.20 Determination of Urbach energy (E_u).....	24
Figure.I.21 Schematic diagram of the Scanning Electron Microscop..	25
Figure.I.22 Schematic diagram of the Four-Point Probe used to determine the electrical resistivity of the TiO_2 thin film , on a glass substrate.....	27
Figure.II.1 structure of anatase.....	29
Figure.II.2 (a) Structure of the brookite phase of TiO_2 , (b) the arrangement of the constitutive octahedron of brookite.....	29
Figure.II.3 structure of rutile.....	30
Figure.II.4 Phase transition of titanium dioxide.....	33
Figure.II.5 Molecular-orbital bonding structure for anatase TiO_2 : (a) atomic levels, (b) crystal-field split levels, (c) final interaction states. The thin-solid and dashed lines represent large and small contributions, respectively.....	34
Figure.II.6 Processes occurring on bare TiO_2 particles after UV excitation	35
Figure.II.7 Mechanism of photo-induced hydrophilicity	35
Figure.II.8 Applications of TiO_2	37
Figure.III.1 Spin coating.....	38
Figure.III.2 Glass substrates.....	42
Figure.III.3 Schematic represents the experimental procedure.....	43
Figure.III.4 Photograph of our five films prepared with different solvents.....	43
Figure.III.5 Simple test of adhesion.....	44
Figure.III.6 The variations of the thickness as a function of solve.....	45

Figure.III.7 Schematic illustration of the impact of boiling point on the colloidal size distribution in solutions.....	46
Figure.III.8 Reference sheets (JCPDS) specific toTiO ₂	47
Figure.III.9 X-ray diffraction patterns of TiO ₂ thin films.....	47
Figure.III.10 The variations of crysstallite size as a function of solvents.....	49
Figure.III.11 Structural parameters of TiO ₂ thin films with different solvent.....	51
Figure.III.12 The transmittance spectra of TiO ₂ films deposited using different solvent.....	52
Figure.III.13 The band gap indirect approximation using Tauc's plot.....	53
Figure.III.14 The band gap direct approximation using Tauc's plot.....	54
Figure.III.15 The variation of the optical gap energy (direct and indirect) and the thickness of TiO ₂ thin films with different solvent.....	54
Figure.III.16 The variation of the optical gap energy (direct and indirect) and the Urbach energy of TiO ₂ thin films with different solvent.....	55
Figure.III.17 SEM images of TiO ₂ thin films with different solvent.....	56
Figure.III.18 Energy dispersive spectra of TiO ₂ preparedwith different solvent.....	58
Figure.III.19 The variation of the Resistivity and thickness of Prepared with different solvents TiO ₂ films.....	60

List of Tables

Table.II.1 Comparison of the rutile, anatase and brookite, different crystal structures of TiO ₂	31
Table.III.1 The properties of the solvents.	40
Table.III.2 The thickness of TiO ₂ thin films deposited using different solvents.....	45
Table.III.3 The Variation of crystallite size according to solvents.....	49
Table.III.4 The Variation of dislocation density and deformation according to solvents.....	50
Table.III.5 The Optical gap variations (direct , indirect).....	53
Table.III.6 Variation of the Urbach energy as a function of the Solvents.....	55
Table.III.7 Resistivity and conductivity of Prepared with different solvents TiO ₂ films.....	60

Introduction General

Nowadays, most of the technologies are used for minimizing the materials into nano-size as well as nano-thickness leading to the emergence of new and unique behaviors of such materials in optical, electrical, optoelectronic, dielectric applications, and so on. Hence, a new branch of science/materials science is called thin films or coatings[1].

Transparent conducting films have attracted much attention due to their large scale application as electrodes for the development of liquid crystal displays, plasma display panels, organic electroluminescence, solar cells, etc. The properties requested by these films in the view of such applications are: high transmittance in the visible range, high electrical conductivity when the film is UV excited and high thermal stability. From this point of view TiO_2 is a fascinating material due to its wide-ranging chemical and physical properties like high chemical stability, high efficiency in organic and inorganic pollutants photo-decomposition, high catalytic activity, biocompatibility and non-toxicity as well as to its low production cost[2].

Thus TiO_2 is one of the most widely used materials in various applications, and to obtain the thin layers of TiO_2 , different deposition techniques have been used among the techniques using the sol-gel technique, sol-gel method has the advantages of simplicity, inexpensiveness, low temperature processing, the ability to form homogeneous multicomponent films on large areas, non-vacuum processing, possibility to form porous film.

Several researchers have been reported that the performance of the sol-gel method significantly depends on the process conditions such as water/ alkoxide ratio, pH, type of precursors and reagents, reaction and mixing conditions . However, to the best of our knowledge, little attention has been devoted to the effects of solvent type on the structural optical and electrical properties of the TiO_2 thin films prepared by the sol-gel method. Therefore additional studies are needed to investigate the effect of solvent type on the properties of TiO_2 thin films. The aim of this work is to improve the Structural, optical and electrical properties of TiO_2 thin films[3].

The work described in this memory is presented in 3 chapters, as follows:

The first chapter will deal, the thin film most important deposition techniques and tools of characterizations (Structural, Electrical and Optical) and different methods of the deposit characteristics calculation (the crystallite size, the thickness, the optical gap, and Disorder...) will be discussed. In second chapter will include bibliographic research on titanium oxide, its properties and its applications.

In the third chapter, will present the description of the various stages in the development of thin films of titanium oxide by the sol-gel method and summarizes obtained experimental results of this work concerning the effect of different solvents and the corresponding discussions.

In the end, we finish our work with a general conclusion and some tracks to complete.

Chapter I:

Thin films deposition and characterization
techniques.

In this chapter, we talk about the most important methods of chemical deposition "sol-gel", the most important method used to apply sol-gel on substrate "spin coating". Then , we talk about the used technique for characterizing of our samples.

I.1 Thin film technology

Thin film can be defined as a thin layer of material, where the thickness is varied from several nanometers to few micrometers. Like all materials, the structure of thin films is divided into amorphous and polycrystalline structure depending on the preparation conditions as well as the material nature. Thin films comprise two parts: the layer and the substrate where the films are deposited on it. Also, thin films can be composed of different layers such as thin film solar cells, electrochromic cells, and so on[1].

I.1.1 This film feature

Thin films are generally used to improve the surface properties of solids. Transmission, reflection, absorption, hardness, abrasion resistance, corrosion, permeation and electrical behaviour are only some of the properties of a bulk material surface that can be improved by using a thin film. Nanotechnology also is based on thin film technology[4].

I.1.2 Formation stages of thin films

In a large number of deposition techniques, thin films growth is by atom by atom (or molecule by molecule). The formation of the thin films is divided into four stages [5]:

- a) Nucleation, during which small nuclei are formed that are statistically distributed (with some exceptions) over the substrate surface.
- b) Growth of the nuclei and formation of larger islands, which often have the shape of small crystals (crystallites).
- c) Coalescence of the islands (crystallites) and formation of a more or less connected network containing empty channels.
- d) Filling of the channels.

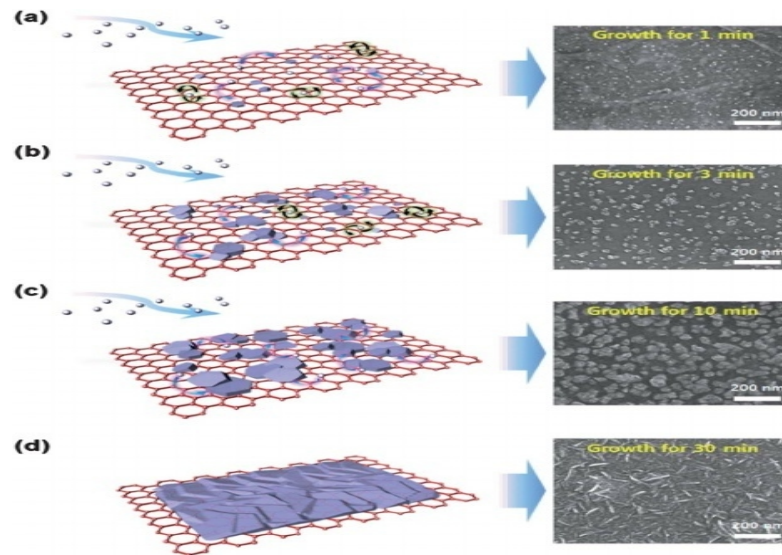


Figure.I.1 Schematics and FE-SEM images of the stages of thin film growth[6].

I.1.3 Thin film growth modes

- a) 2D or layer-by-layer growth, also known as **Frank-Van DerMerwe(FVDM)** mode. The condensing particles have a strong affinity for the substrate atoms: they bond to the substrate rather than to each other .
- b) 3D or island growth mode, also known as **Volmer-Weber(VW)** mode. The datoms have a strong affinity with each other and build 3D islands that grow in all directions, including the direction normal to the surface. The growing islands eventually coalesce and form a contiguous and alter continuous film.
- c) A mixed mode that starts 2D growth that swithes into island mode after one or more monolayers; this mode is also known as **the Stranski-Krastanov (SK)** mode[7].

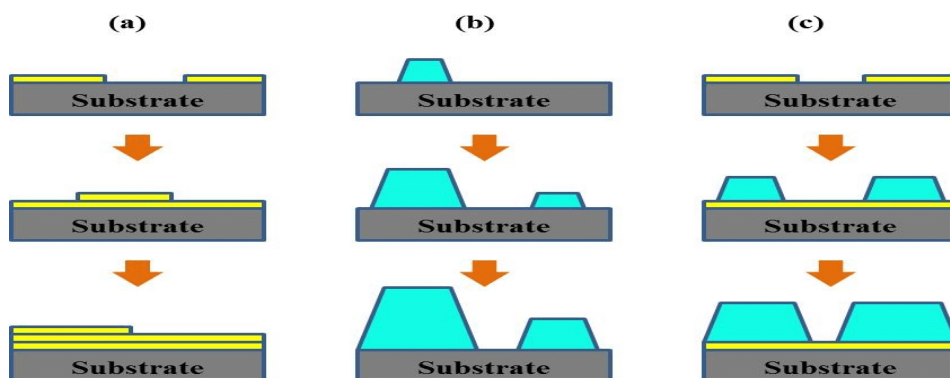


Figure.I.2 Schematic diagram of three basic growth modes: (a) Frank-Van DerMerwe, (b) Volmer-Weber(VW) , (c) the Stranski-Krastanov (SK) [8].

I.2 Deposition techniques

Depending on the desired application, well-controlled thin material films can be deposited either by physical or chemical protocols, following top-down or bottom-up approaches (**Figure.I.3**).

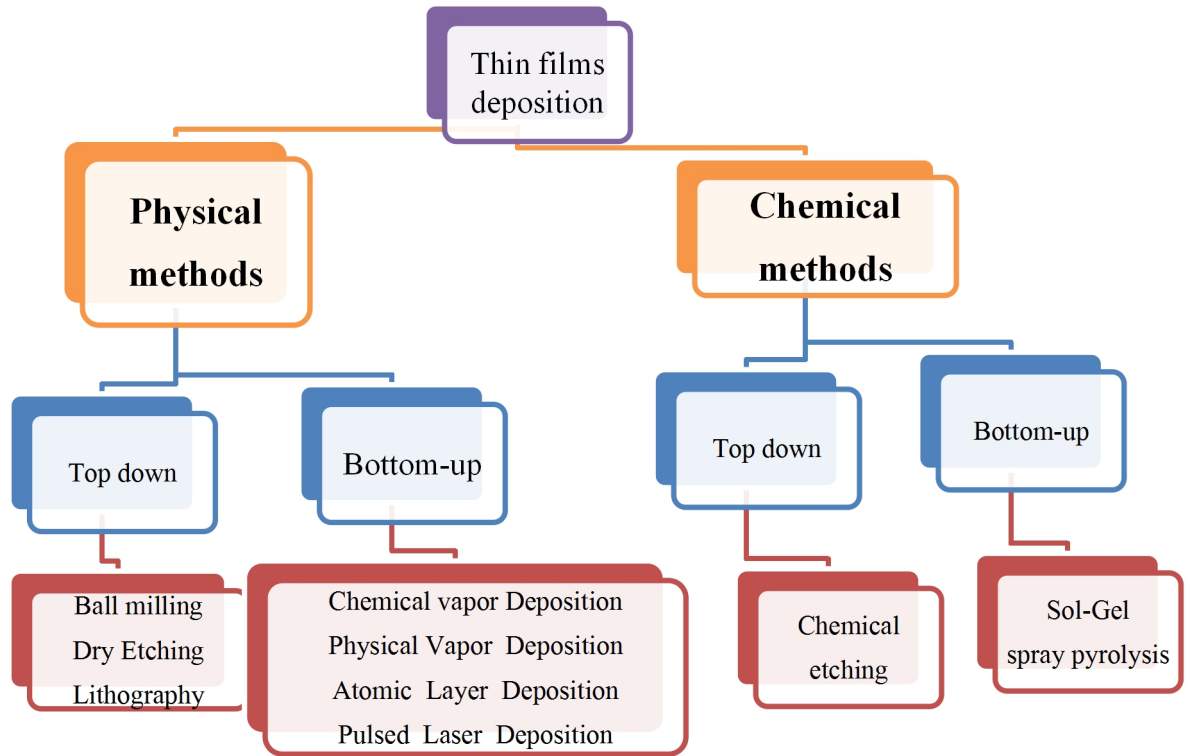


Figure.I.3 Thin films deposition techniques[9].

- **“bottom-up” method:** This method allows the assembly or the positioning of atom or molecules in a precise way thus allowing the manufacture of materials whose structure is perfectly controlled. This method uses mainly physical and chemical processes.
- **“top down” method:** This method involves miniaturizing the current systems. The structures are thus gradually under dimensioned until reaching nanometric proportions. This method uses mainly mechanical processes[10].

I.2.1 Sol-gel technology

Sol-gel offers many attractive advantages over conventional ways of producing oxide materials. These include the possibility of varying the film properties extensively by changing the composition of the solution (to produce change in film microstructure) and a relatively low process cost. In addition, sol-gel overcomes the difficulties of producing a high quality dielectric-semiconductor interface, and obtaining a stoichiometric ratio of elements and

molecular homogeneity in multicomponent oxide films. There are many forms in which the oxide gel product can be produced. These include powders, coatings, monoliths and fibres (**Figure.I.4**) which often require very low processing temperatures. The possibility of the use of high purity starting materials and the ease with which large and complex shaped substrates can be coated has meant that this technique is becoming increasingly attractive to optoelectronic specialists. The need for low-cost thin film production processes has increased the interest in sol-gel (and other non-vacuum deposition techniques) capable of deposition at high rates and over larger areas[11].

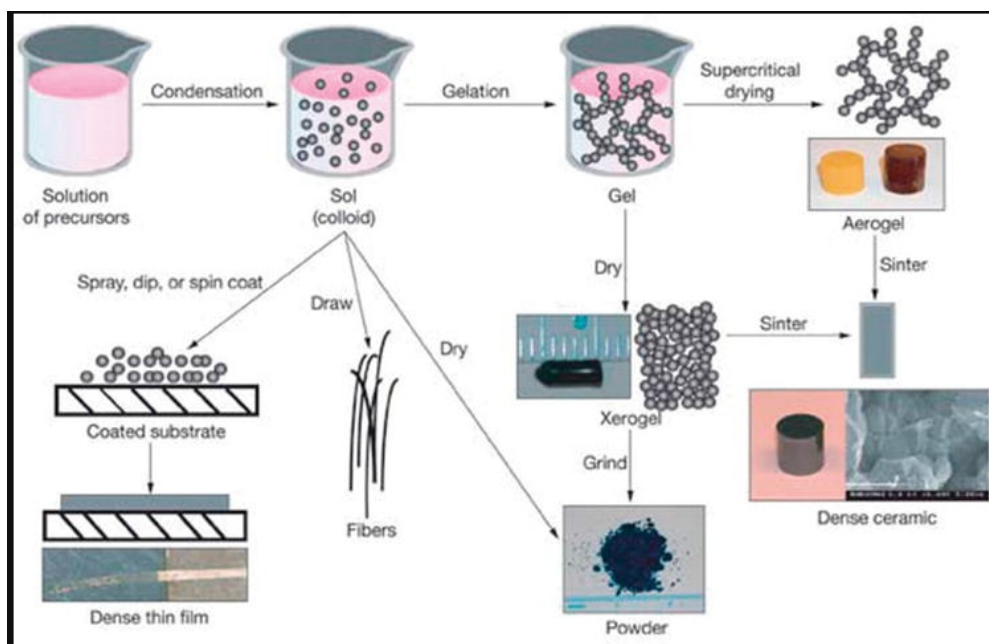


Figure.I.4 Stages of the sol-gel process[12].

I.2.2 Sol-gel method

The sol-gel technique is broadly used for the synthesis of oxide materials. Sol-gel process is one of the famous wet-chemical methods. It works under lower-temperature processing and gives better homogeneity for multicomponent materials. The word "sol" means the formation of a colloidal suspension and 'gel' means the conversion of 'sol' to viscous gels or solid materials. Two routes are used to prepare transition metal oxides (TMOs) as follows[1]:

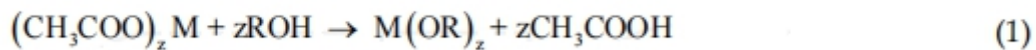
- a) Preparing of inorganic precursors via inorganic salts in aqueous solution.

b) Preparing of metal alkoxide precursors via metal alkoxides in nonaqueous solvents.

In this section, we are concerned on the famous route “ the metal alkoxide precursor solution by an alcoholic solution ”.

- A **sol** is a stable suspension of colloidal particles (nanoparticles) in a liquid. The particles can be amorphous or crystalline, and may have dense, porous, or polymeric substructures. The latter can be due to aggregation of subcolloidal chemical units[13].
- The **gel** is a kind of solid feature of the colloidal system composed of fine particles in three-dimensional network structure and a continuous medium consisting of dispersed phase. The transition process to the gel can be briefly described as the formation of the polymer or the particle aggregates formed by the condensation reaction into a small particle cluster and gradually connected to a three-dimensional network structure. Therefore, the gelation process can be regarded as a small particle cluster connected to each other as a continuous solid network[14].
- **Alkoxide precursors in organic solvents**

The sol-gel technique is based on the polycondensation of metal alkoxides $M(OR)_z$ in which R represents an alkyl group ($R = CH_3, C_2H_5, \dots$) and z is the oxidation state of the metal atom M^{z+} . It can be synthesized via the reaction of metal salt (chloride, acetate, nitrate, etc.) with alcohol as follows[1]:



After this process, two important steps should be involved:

➤ **Hydrolysis**: this step is aimed to form reactive **M-OH** groups:

A non-ionized molecular precursor reacts with water, such as a metal alkoxide $M(OR)$ [15].

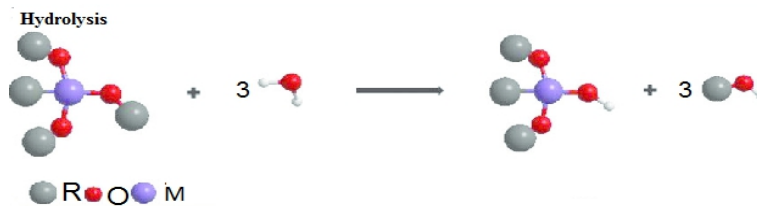


Figure.I.5 Sol-gel reactions of organically modified alkoxide precursors (Hydrolysis)[16].

➤ **Condensation:** condensation is the second step after hydrolysis leading to the departure of a water molecule. The process of condensation can be either olation process or oxolation process[1].

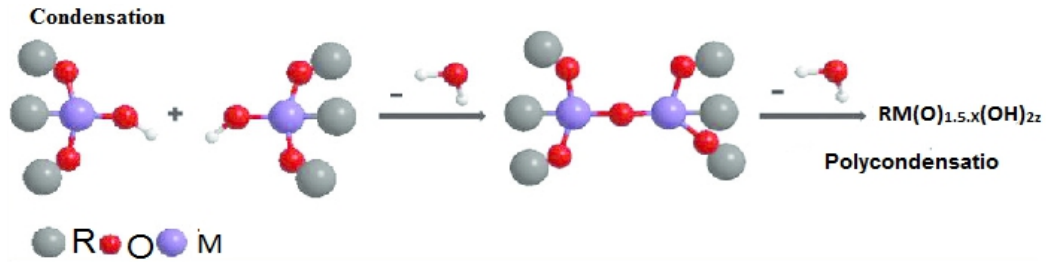


Figure.I.6 Sol-gel reactions of organically modified alkoxide precursors (Condensation)[16].

Olation: a hydroxyl bridge ("ol" bridge) is formed between two metal centers as shown in Figure.I.7.

Oxolation: oxolation is a reaction in which an oxo bridge (—O—) is created between two metal centers. When the metal is coordinately unsaturated, oxolation with rapid kinetics leads to edge- or face-shared polyhedral as shown in Figure.I.8.

Hence, olation process occurs mainly for lower oxidation states of cations ($z < 4$), whereas oxolation is mainly observed with cations of high oxidation state ($z > 4$).

The previous description provides the preparation of the precursor solution. In order to make thin film from the precursor solution, there are two processes for the production of the films that is, dip-coating and spin-coating techniques[1].

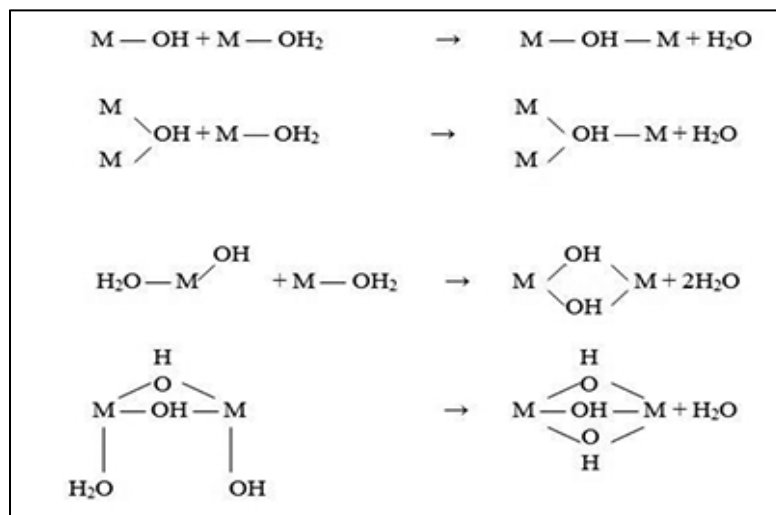


Figure.I.7 Several types of OH bridges can be formed by olation condensation process.

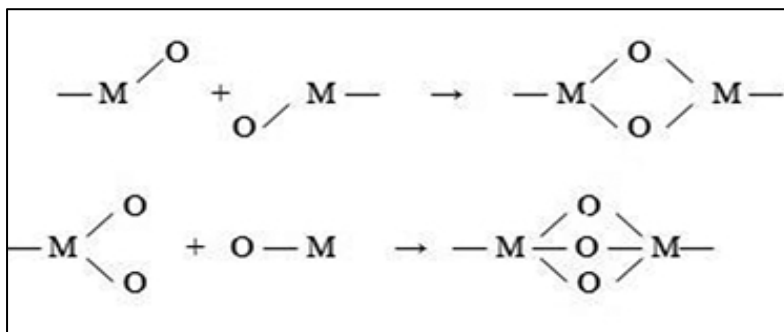


Figure.I.8 Formation of oxo-bridging links between two metal centers.

I.2.2.1 Sol-gel chemistry tends to be particularly sensitive to the following parameters

I.2.2.1.1 Precursor properties

Metal ion radius, electronegativity, coordination number, etc., all affect the nature of the metal alkoxide in the solvent. The hydrolysis and polycondensation reaction are determined by the number of partial positive charges of the metal atom and the ability of the metal atom to increase its coordination number. The coordination number increases strongly as the positive charge of a metal atom increases, and the reaction rate is faster[15].

I.2.2.1.2 Reaction temperature

The chemical kinetics of the different reactions involved in the formation of nanoparticles and the assembly of the nanoparticles in a gel network are accelerated with temperature, which affects the gel time. At very low temperatures, gelation is a slow process that can take weeks or months. In contrast, at high temperatures, the reactions that bind the nanoparticles to the gel network occur so quickly that lumps form in their place and a solid precipitates out of the liquid. The gelation temperature must be controlled to optimize the reaction time[17].

I.2.2.1.3 Gel time

Depending on the type of gel to be obtained, the different steps in the gel formation process work differently at different time scales. In general, it is recommended that the formation of the gel should be slow to produce a very uniform structure, resulting in a

stronger gel. Accelerating reactions through short times cause precipitates to form instead of gel network and can cause a gel to become cloudy and weak or simply not form[17].

I.2.2.1.4 Solvent

In the polymerization process, as molecules are assembled into nanoparticles, the solvent plays two important roles; the first is that it must be able to keep the dissolved nanoparticles so that they do not precipitate out of the liquid; and second, it must play a role in helping nanoparticles connect with each other [17]. **The activity of alkoxide hydrolysis is changed due to the exchange of the -OR groups in the alkoxide with -OR' groups in the alcohol solvent.** Hence, depending on the selected solvent, the rate of hydrolysis and gelation time of the same alkoxide may vary. Drying of wet gels is also affected by the solvent type. The rate of drying is higher when the saturated vapor pressure of the solvent is high but this may cause cracking of the gel[15].

I.2.2.1.5 Properties and concentrations of catalyst

The use of catalysts can increase the rate of hydrolysis and the hydrolysis is more thorough. The most commonly used catalysts are acetyl acetone and diethanolamine [15].

I.2.2.1.6 Ratio of water to metal alkoxide

The ratio of the amount of water to precursor is measured by the water amount and is represented usually by the symbol R . It directly influences the structure of the alkoxide-hydrolyzed polycondensation product. The molecules of alkoxide are less hydrolyzed alkoxys due to the less amount of water which is the formation of hydroxyls by less hydrolysis, and a low degree of crosslinking is produced by the polycondensation between the partially hydrolyzed alkoxide molecules. On the contrary, a highly cross-linked product is easily formed with more amount of water. The quantity of water is also meticulously connected to the viscosity and gelation time of sol. An increase in R leads to an increase in the viscosity of the sol and the shortening of gelation time due to the fact the amount water is less than the stoichiometric amount of water (N) required for hydrolysis. Since the water amount maximizes the degree of crosslinking, the degree of polymerization of the polycondensate also increases. However, when the water quantity exceeds N , with increasing R the viscosity will be reduced and the gelation time will be prolonged due to the excess amount of water reducing the concentration of polycondensate. Additionally, an excess amount of water also

affects the subsequent drying process in causing shrinkage and drying stress of gels and prolonging the drying time[15].

I.2.2.2 The relationship between gel time and reaction temperature

The rate of hydrolysis of alkoxides accelerates as the reaction temperature increases. To reduce the reaction time alkoxides (such as silicon alkoxide) are often manipulated under heating due to their low hydrolysis activity[15], the time required to form a gel decreases as the temperature is increased [18].

I.2.2.3 Advantages of sol-gel method

Sol-gel delivery systems show several advantages, among which:

- ✚ **Versatile Versatile:** better control of the structure, including porosity and particle size, possibility of incorporating nanoparticles and organic materials into sol-gel-derived oxides.
- ✚ **Extended composition ranges extended composition ranges:** it allows the fabrication of any oxide composition, but also some non-oxides, as well as the production of new hybrid organic-inorganic materials, which do not exist naturally.
- ✚ **Better homogeneity:** due to mixing at the molecular level, high purity.
- ✚ **Less energy consumption less energy consumption:** there is no need to reach the melting temperature, since the network structure can be achieved at relatively low temperatures near T_g .
- ✚ No need for special or expensive equipment.
- ✚ It does not need high temperature and gives good thickness compared to thin film deposition methods(Figure.I.9)[19].

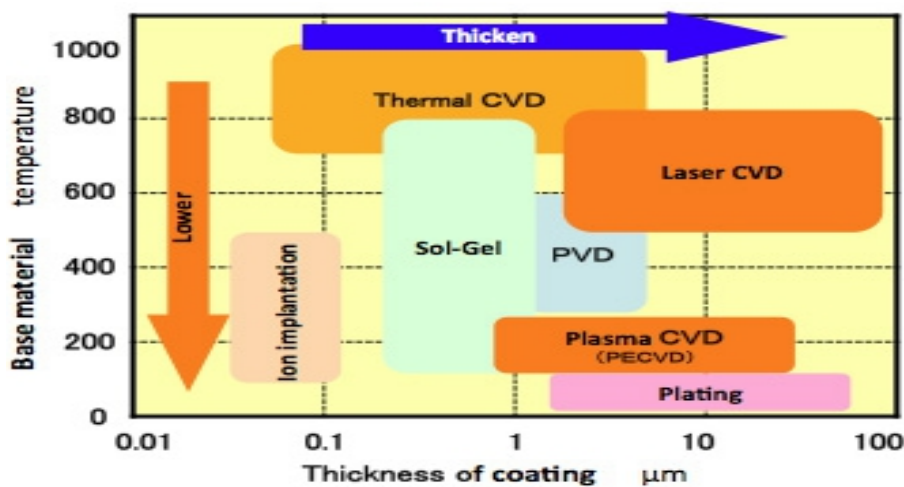


Figure.I.9 Technical trends of thin films[20].

I.3 Methods used to apply sol-gel on substrates

Probably one of the greatest advantages of the sol-gel technique over other film deposition methods is its versatility. Prior to gelation, the sol can be spin-coated, dip-coating, electrodeposition. Each of these methods has respective advantages and drawbacks(**Figure.I.10**).

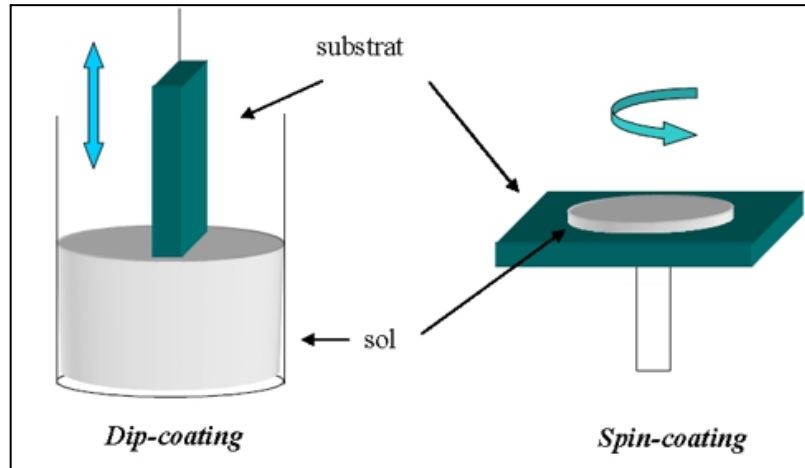


Figure.I.10 Preparation of coatings by sol-gel method [21].

I.3.1 Spin coating

Spin coating is widely used in microfabrication of functional oxide layers on glass or single crystal substrates using sol-gel precursors, where it can be used to create uniform thin films with nanoscale thicknesses.

I.3.1.1 Description of spin coating process

There are four distinct stages to the spin coating process. These include:

a) dispense stage

A typical spin process consists of a dispense step in which the resin fluid is deposited onto the substrate surface as in Figure.I.11 (a). Two common methods of dispense are static dispense, and dynamic dispense. Static dispense is simply depositing a small puddle of fluid on or near the center of the substrate. This can range from 1 to 10 cc depending on the viscosity of the fluid and the size of the substrate to be coated. Higher viscosity and or larger substrates typically require a larger puddle to ensure full coverage of the substrate during the high speed spin step. Dynamic dispense is the process of dispensing while the substrate is

turning at low speed. A speed of about 500 rpm is commonly used during this step of the process. This serves to spread the fluid over the substrate and can result in less waste of resin material since it is usually not necessary to deposit as much to wet the entire surface of the substrate. This is a particularly advantageous method when the fluid or substrate itself has poor wetting abilities and can eliminate voids that may otherwise form [22].

b) Substrate acceleration stage

This stage is usually characterized by aggressive fluid expulsion from the wafer surface by the rotational motion. Because of the initial depth of fluid on the wafer surface Figure.I.11 (b), spiral vortices may briefly be present during this stage; these would form as a result of the twisting motion caused by the inertia that the top of the fluid layer exerts while the wafer below rotates faster and faster. Eventually, the fluid is thin enough to be completely co-rotating with the wafer and any evidence of fluid thickness differences is gone. Ultimately, the wafer reaches its desired speed and the fluid is thin enough that the viscous shear drag exactly balances the rotational accelerations.

Typical spin speeds for this stage range from 1500-6000 rpm, again depending on the properties of the fluid as well as the substrate. This step can take from 10 seconds to several minutes. The combination of spin speed and time selected for this stage will generally define the final film thickness. In general, higher spin speeds and longer spin times create thinner films. The spin coating process involves a large number of variables that tend to cancel and average out during the spin process and it is best to allow sufficient time for this to occur [22].

c) A stage of substrate spinning at a constant rate and fluid viscous forces dominate fluid thinning behaviour

This stage is characterized by gradual fluid thinning. Fluid thinning is generally quite uniform (as in Figure.I.11 (c)), though with solutions containing volatile solvents, it is often possible to see interference colours “spinning off”, and doing so progressively more slowly as the coating thickness is reduced. Edge effects are often seen because the fluid flows uniformly outward, but must form droplets at the edge to be flung off. Thus, depending on the surface tension, viscosity, rotation rate, etc..., there may be a small bead of coating thickness difference around the rim of the final wafer . Mathematical treatments of the flow behaviour

show that if the liquid exhibits newtonian viscosity (i.e., is linear) and if the fluid thickness is initially uniform across the wafer (albeit rather thick), then the fluid thickness profile at any following time will also be uniform leading to a uniform final coating [22].

d) A stage of substrate spinning at a constant rate and solvent evaporation dominates the coating thinning behavior

As the prior stage advances, the fluid thickness reaches a point where the viscosity effects yield only rather minor net fluid flow. At this point, the evaporation of any volatile solvent species will become the dominant process (**Figure.I.11(d)**) occurring in the coating. In fact, at this point the coating effectively “gels” because as these solvents are removed the viscosity of the remaining solution will likely rise effectively freezing the coating in place.

After spinning is stopped many applications require that heat treatment or “firing” of the coating be performed (as for “spin-on-glass” or sol-gel coatings). On the other hand, photoresists usually undergo other processes, depending on the desired application/use.

Clearly stages (c) and (d) describe two processes that must be occurring simultaneously throughout all times (viscous flow and evaporation). However, at an engineering level the viscous flow effects dominate early on while the evaporation processes dominate later[22].

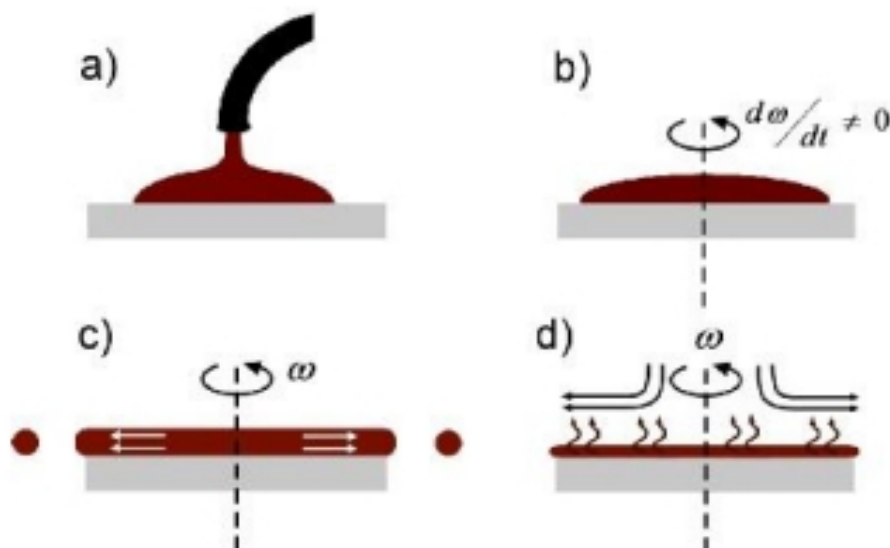


Figure.I.11 Four distinct stages to spin coating[20].

I.3.1.2 Thin films characteristics

The thin film thickness is depends on three important parameters. They are speed, viscosity of solution, and evaporation. First we consider speed with film thickness. The thickness of the film is inversely proportional to the square root of the speed of the disk and it is given by[23].

$$t \propto \frac{1}{\sqrt{\omega}}$$

Where t is the thickness of the thin film and ω is the spinning speed of the substrate. The graph shown below (**Figure.I.12**) gives relationship about film thickness and speed. From this it is clearly observed that the increase in speed, reduces the film thickness.

Now considering the next parameter which is viscosity and concentration of solution. Viscosity means fluid resistance. If these in high value, then it is hard to the solution to spread all over the substrate and will affect uniformity and thicker film. So, it should be maintained by constant while preparing the solution itself. Then the last parameter is rate of evaporation. If the solvent of the solution is not evaporated properly or time taken for evaporation is increased means the viscosity and concentration of solution is increased which result in thicker film. So, solvent should evaporate as soon as in room temperature otherwise separate annealing process should be given at the fourth phase. Hence, to get the desired thin film, these three parameters should be considered or satisfied as we discussed[23].

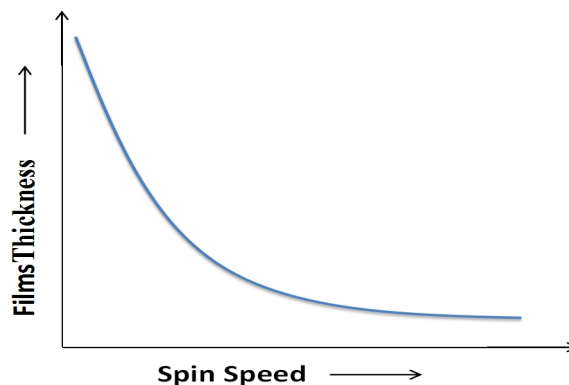


Figure.I.12 Relation between film thickness Vs speed[23].

I.3.1.3 Advantages disadvantages of spin coating

The main advantages of spin coating are:

- The simplicity and relative ease with which a process can be set up coupled with the thin and uniform coating that can be achieved at various thicknesses makes it ideal for both reasearch and rapid prototyping.
- The ability to have high spin speeds leads to fast drying times (due to the high airflow) which in turn results in high consistency at both macroscopic and nano length scales, and often removes the need for post-desposition heat treatment.
- Spin coating is a very low cost way to batch process individual substrates compared to other methods, many of which require both more expensive equipment and high energy processes.
- The thin film thickness can be change easily by changing the spin speed of the spin coater or change the viscosity of the liquids[24].

I.3.2 Drying

Thin film drying typically takes place in an oven or on a hot plate ranging from room temperature to 300 °C. For temperatures greater than 100 °C, a large percentage of the thin film weight is lost, as the solvent quickly evaporates. After achieving a desired thickness, the thin film is subject to other forms of thermal treatment at higher temperatures in more controlled atmospheres[25].

I.3.3 Annealing

Thermal annealing is an usual process used for intrinsic stress liberation, structural improving, and surface roughness control in materials. Annealing of the samples is performed so as to improve the crystallinity of the thin films and also to recover the local stresses and to evaporate the remaining[26].

I.4 Thin film characterization

I.4.1 X-ray diffraction

X-rays were discovered by a German physicist Wilhelm Conrad Röntgen in 1895. X-rays are electromagnetic waves with high frequency and short wavelengths ranging in the

order of 1×10^{-4} and 1 \AA . Their comparable size to atoms allows to measure interatomic distances in crystalline structured materials. In 1912, von Laue discovered that the crystals diffract X-rays. X-ray diffraction (XRD) is a powerful tool to reveal information about crystal structure, plane spacing, particle size, lattice constants and chemical compositions.

The generated X-rays interact with the electrons in an atom. At a certain angle, if the interference of reflected beams from various planes is constructive, diffracted beam is observed as seen in Figure.I.13. The peak intensity of an XRD scan defines the diffracted beam due to constructive interference. The spacing between crystal planes is determined by Bragg's Law as follows:

$$n\lambda = 2d_{(hkl)} \sin \theta_{(hkl)} \quad (I.1)$$

Where n is an integer, λ is the wavelength of monochromatic X-ray source, (hkl) are the Miller indices that define lattice planes, d is the spacing between the planes and θ is the incident angle [27].

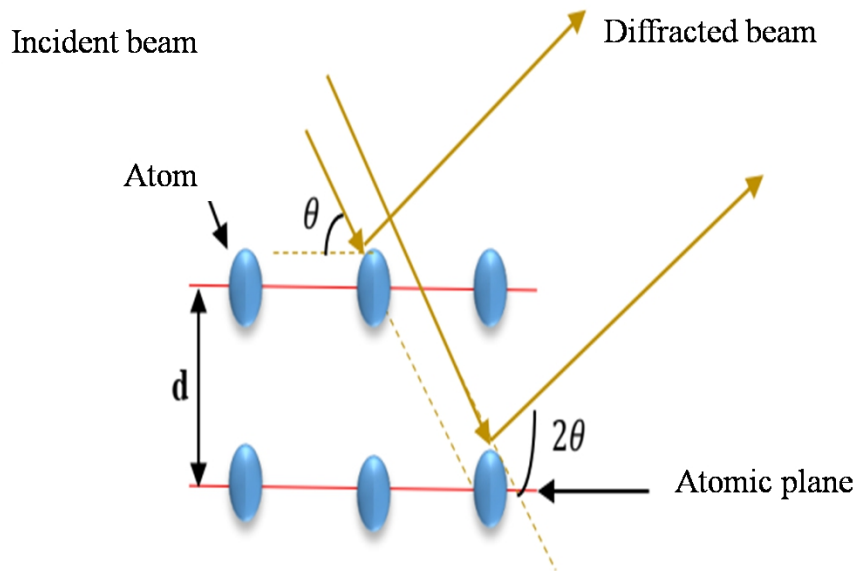


Figure.I.13 Principle of Bragg's law [28].

The diffracted radiation is detected by the counter tube, which moves along the angular range of reflections. The intensities are recorded on a computer system. The X-ray diffraction data thus obtained is printed in tabular form on paper and is compared with Joint Committee

Power Diffraction Standards (JCPDS) data to identify the unknown material. The sample used may be powder, single crystal or thin film as used in the present studies[28].

I.4.1.1 Determination of the crystallite size

The crystallite size of the elaborated sample is estimated from the full width at half maximum (FWHM) of the most intense diffraction line by Scherrer's formula as follows[29]:

$$D = \frac{0.9\lambda}{\beta \cos \theta} \quad (I. 2)$$

D: The crystallite size (nm).

λ : The wavelength of X-ray (nm).

β : The full width at half maxima of the peak (FWHM) in radians.

θ : The Bragg's angle (rd).

I.4.1.2 Determination the dislocation density

The dislocation density of the crystal gives information about the crystal structure. The smaller the dislocation density better is the crystallization of the film. Dislocation is an imperfection in a crystal associated with misregistry of the lattice in one part of the crystal with respect to another part., dislocation density (**δ**) is a measure of lattice imperfections and defects[30], and It can be can be calculated using the grains size values according to the following relation [29]:

$$\delta = \frac{1}{D^2} \quad (I.3)$$

I.4.1.3 Determination of the deformation

To calculate the deformation using the following relation[31]:

$$\varepsilon = \frac{\beta \cos \theta}{4} \quad (I.4)$$

Where, **β** : The full width at half maximum intensity of peak in(rad).

θ : The angle of the diffraction peak(rad).

I.4.2 Spectroscopy (UV-VISIBLE)

The optical absorption edge of semiconductor is directly related to band gap where longer wavelength corresponding to bigger band gap, so optical absorption properties were the focus of interest throughout the whole work. The optical properties of transparent samples, including thin film and solution, are usually measured by UV-visible absorption spectrometer, in which one beam of light from ultraviolet or visible light source passes through the sample and then detected by an electronic detector. By comparing the intensity of measured light I with that of reference beam I_0 , the spectrometer gives out the absorption ratio at specific wavelength, which is presented as transmittance ($T=I/I_0$) or absorbance ($A= -\log(I/I_0)$). (principle of operation is represented on Figure.I.14, and the Figure.I.15 presents UV-VIS spectra of TiO_2 thin film). The spectrometer can automatically scan all wavelengths in a given range, providing a curve of absorption versus wavelength of incident beam, For thin film, the absorption coefficient α is given by:

$$\alpha=A/d$$

Where α is the absorption coefficient, A is the absorbance and d is the thickness of the thin film. If the sample to be measured is opaque, a reflectance spectrometer is necessary to be employed where the incident light is absorbed and reflected by the sample[32].

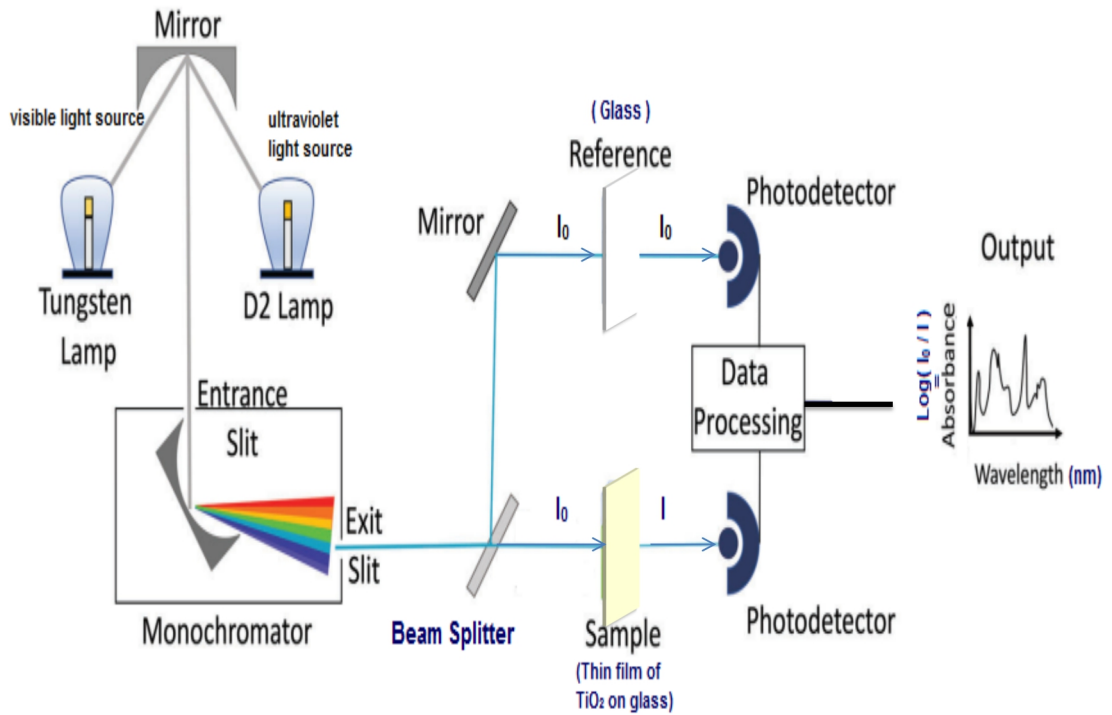


Figure.I.14 Schematic of UV- visible spectrophotometer[33].

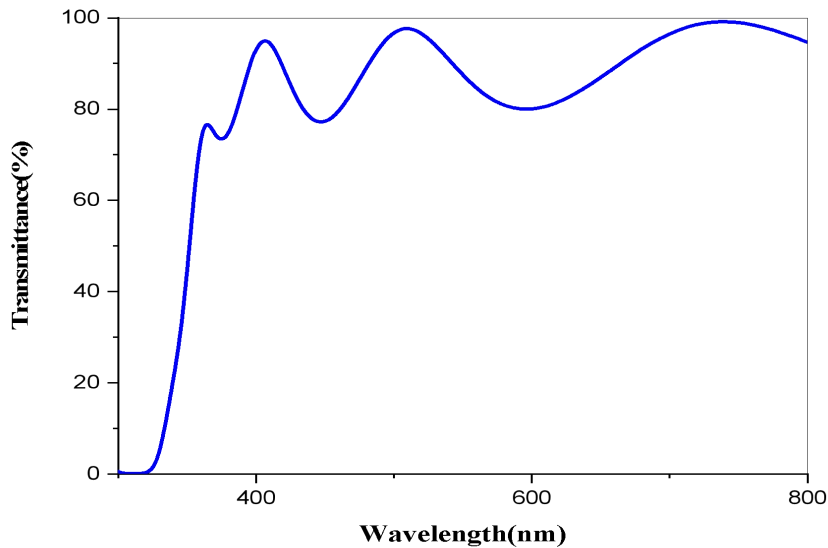


Figure.I.15 Transmittance spectra of TiO₂ thin films.

In addition, thanks to the interferences, one can determine the following parameters: The thickness of the film, the optical gap, and Urbach energy can be calculated using the following relations:

I.4.2.1 The thickness of the film

The physical constants used in calculations are defined in Figure.I.16:

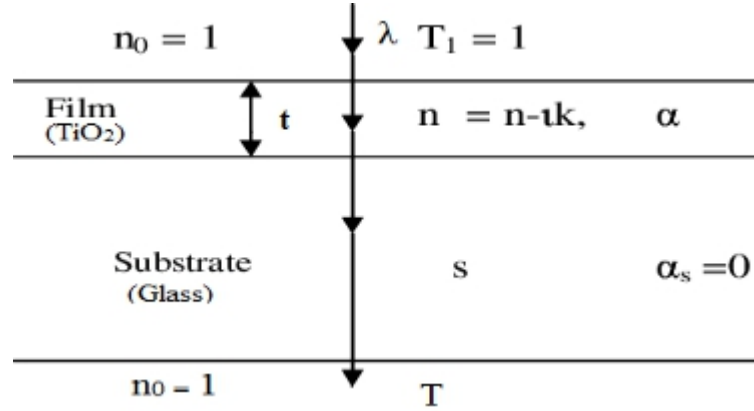


Figure.I.16 System of an absorbing thin film on a thick finite transparent substrate[34].

T is the transmittance, α is the absorption coefficient of film, λ is the incidental light wavelength, n and s are respectively the refraction indexes of the film and the substrate and t represents the film thickness. Using the physical parameters defined in Figure.I.16 and the spectrum of transmission obtained, one can determine the film thickness as follows :

$$t = \frac{\lambda_1 \lambda_2}{2(\lambda_2 n_1 - \lambda_1 n_2)} \quad (I.6)$$

Where: n_1 and n_2 are the refraction index of the film for the wavelength λ_1 and λ_2 we can calculate n_1 and n_2 from the following relation:

$$n_{1,2} = \sqrt{N_{1,2} + \sqrt{(N_{1,2}^2 - s^2)}} \quad (I.7)$$

And $N_{1,2}$ can be obtained using this relation:

$$N_{1,2} = \frac{2s(T_M - T_{m1,2})}{T_M T_{m1,2}} + \frac{(s^2 + 1)}{2} \quad (I.8)$$

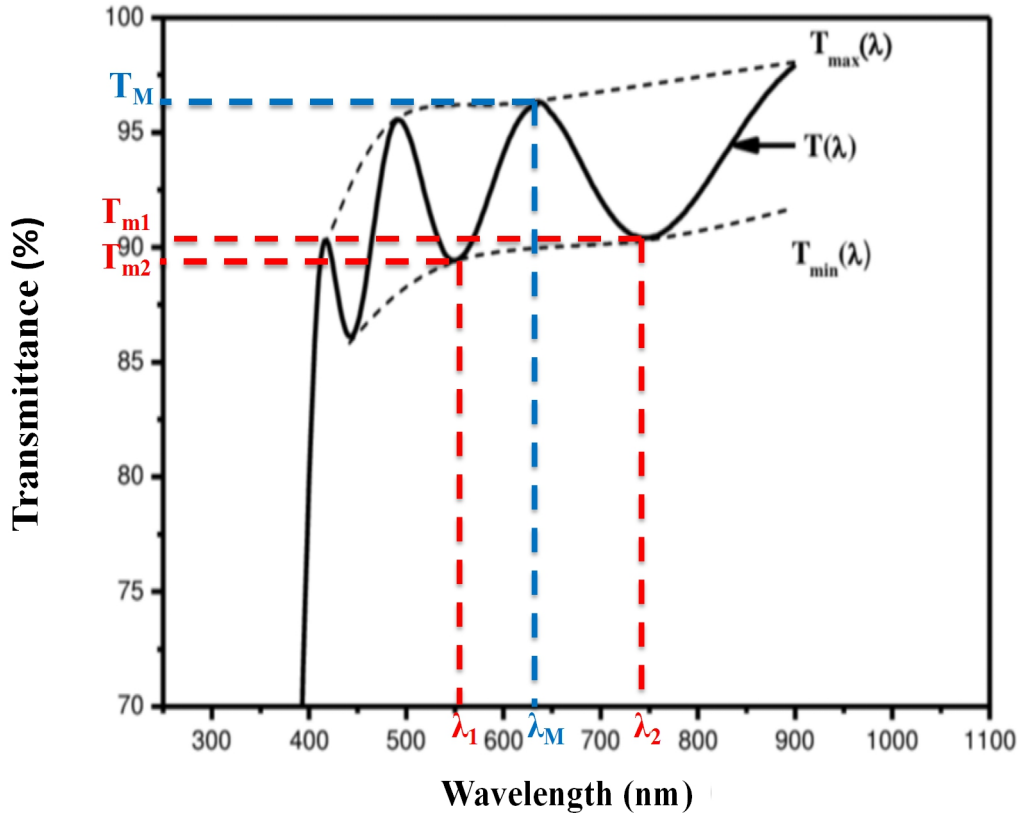


Figure.I.17 Method of interference fringes to determinate the thickness.

I.4.2.2 Optical band gap (E_g)

The fundamental absorption is related to the band-to-band transitions in a polycrystalline semiconductor, i.e., to the excitation of an electron from the valence band to the conductionband. Therefore, the fundamental absorption can be used to determine the energy gap of the semiconductor. The optical band gap (E_g) of films can be estimated using Tauc's formula[35].

$$(\alpha h\nu)^{1/n} = A(h\nu - E_g) \quad (I.9)$$

Where α is the absorption coefficient, A is a constant (independent of photon energy ($h\nu$)), h is the Planck constant and n is the exponent, the value of which is determined by the type of electronic transition causing the absorption and can take the value 1/2 or 2 depending upon whether the transition is direct or indirect, respectively[35].

The indirect bandgap (E_g) are calculated by extrapolating the linear part of the $(\alpha h\nu)^{1/2}$ vs $h\nu$.and the values also of the optical band gap direct are obtained by extrapolating the linear part of the data to the abscissa axis but in the plot of $(\alpha h\nu)^2$ as a function of $h\nu$ as shown in Figure.I.18, Figure.I.19.

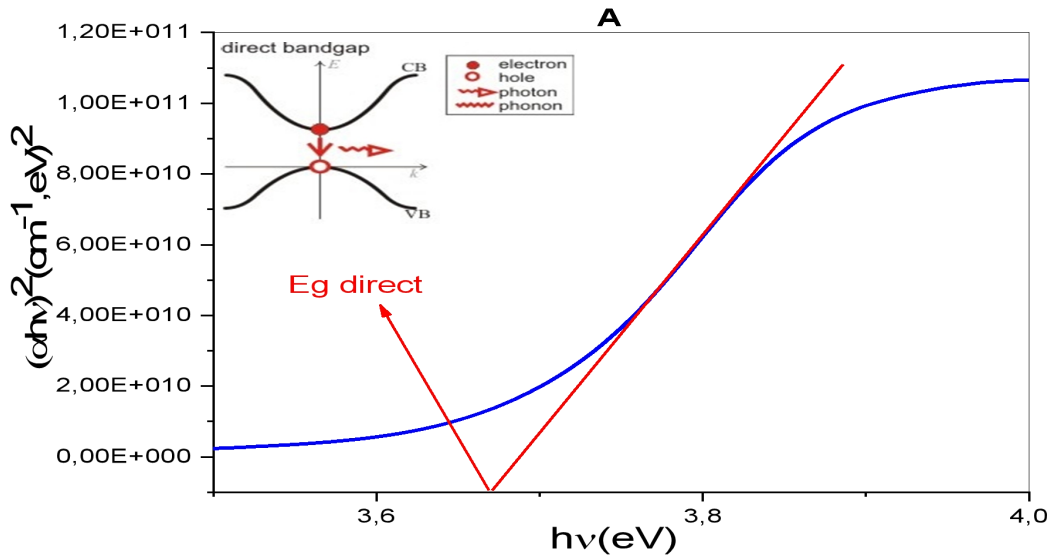


Figure.I.18 Determination of the optical band gap direct (E_g).

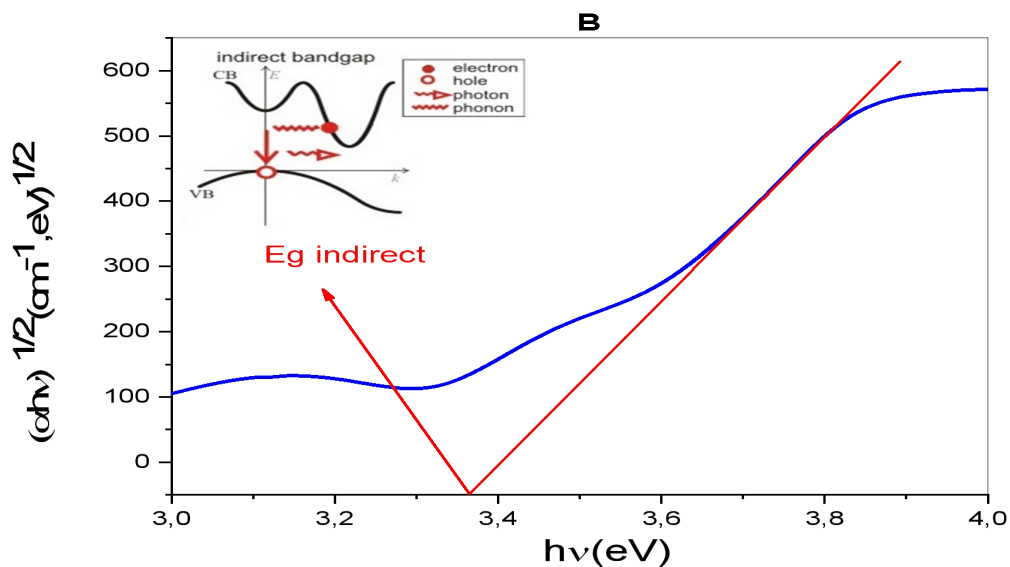


Figure.I.19 Determination of the optical band gap indirect (E_g).

I.4.2.3 Urbach energy (E_u)

Urbach energy is usually used to describe the width of the localized states in the band gap (but not their positions). Pankove has shown that the value of E_u is related to the

impurity concentration. However, redfield has shown that all defects (point, line and planar defects) lead to local electric fields that cause band tailing. Thus, the Urbach energy can be considered a parameter that includes all possible defects. The relation between the Urbach energy and absorption coefficient is described by [36]:

$$\alpha = \alpha_0 \exp\left(\frac{h\nu}{E_u}\right) \quad (I.10)$$

where α_0 is a constant and E_u is Urbach energy.

By drawing $\ln(\alpha)$ versus $h\nu$ we can determine E_u value as the reciprocal of the linear part slope (Figure.I.20):

$$\ln(\alpha) = \ln(\alpha_0) + \frac{h\nu}{E_u} \quad (I.11)$$

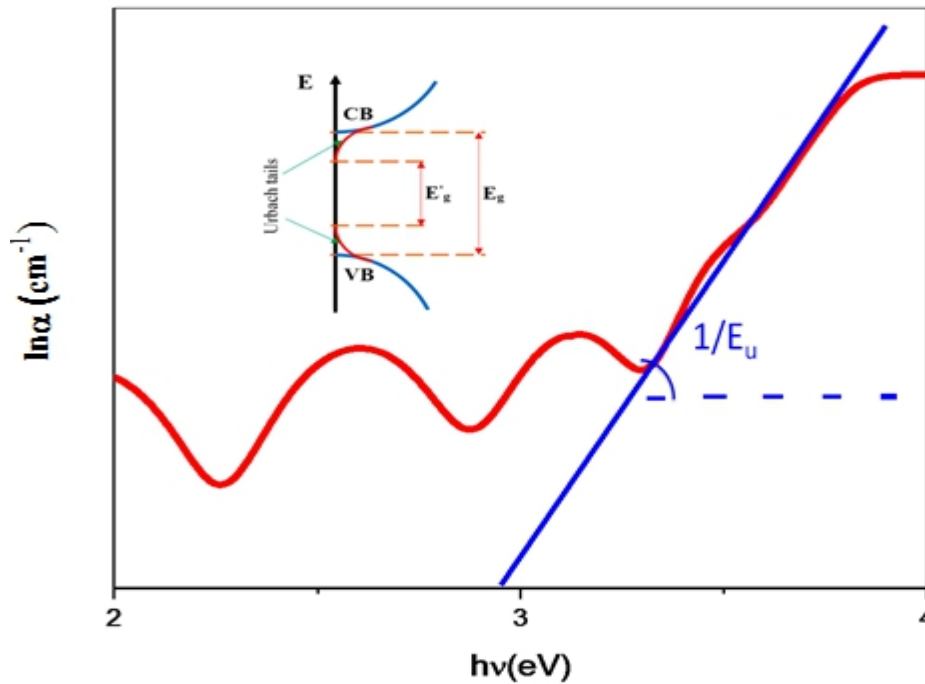


Figure.I.20 Determination of Urbach energy (E_u).

I.4.3 Scanning electron microscopy (SEM)

SEM is useful for detailed study of a specimen's surface. A high-energy electron beam scans across the surface of a specimen, usually coated with a thin film of gold or platinum to improve contrast and the signal-to-noise ratio. As the beam scans across the

sample's surface, interactions between the sample and the electron beam result in different types of electron signals emitted at or near the specimen surface. These electronic signals are collected, processed, and eventually translated as pixels on a monitor to form an image of the specimen's surface topography that appears three-dimensional. Low-energy secondary electrons excited on the sample's surface are the most common signal detected. High-energy backscattered electrons and X-rays are emitted from below the specimen surface, providing information on specimen composition[37].

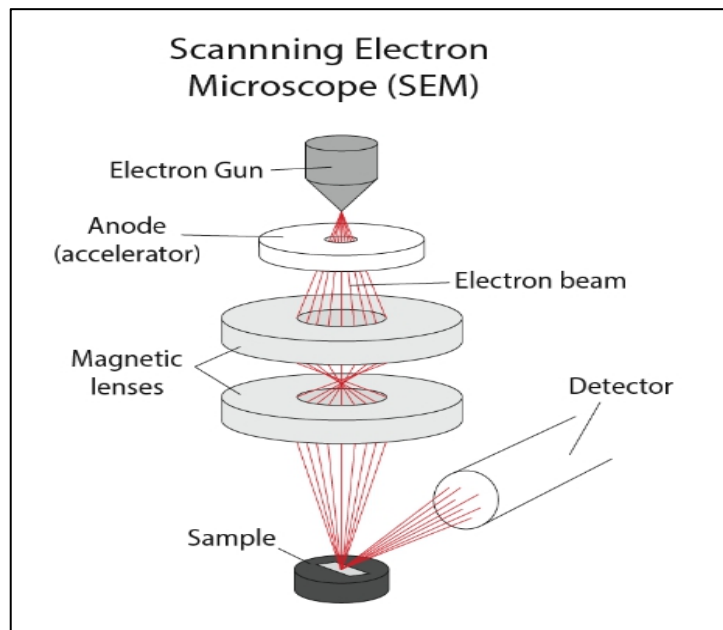


Figure.I.21 Schematic diagram of the Scanning Electron Microscopy[38].

Electron Gun: Electrons are produced by either heating a filament, or by applying a strong electric field to it. Filaments are often made of tungsten, and have a very sharp tip so that a very narrow stream of electrons is emitted.

Anode: The electrons are accelerated down the column of the microscope by the anode. The anode is negatively charged so repels the negatively charged electrons, forcing them to accelerate.

Magnetic lenses: The electrons are focused onto the sample by magnetic lenses. These ensure a very narrow beam of electrons hits the sample.

Sample: The sample scatters the electrons. The amount of scattering (and the number detected at the detector) can depend on many factors, including: sample height, sample

chemistry, and sample crystal structure. X-rays are also produced by the electrons hitting the atoms in the sample. We can analyse these X-rays to tell us which elements exist in the sample.

Detector: The beam is scanned across the sample, and the signal from every point detected. There are many different types of detector that can detect electrons with different energies travelling in different directions. Using different detectors gives us different information about our sample[38].

I.4.4 Four-point probe method

It is a simple and fast method that measures the resistivity of thin layers. It is based on the use of equidistant fourth points (probes) in direct contact with the surface of the sample, placed either linearly or in the form of a square (**FigureI.22**). The principle of the measurement is simple, it is enough to inject a current (I) to the two extreme points and to measure the tension (V) at the two internal points[12]:

When the distance a between the terminals is much greater than the thickness of the thin film, i.e. $t \ll a$ (the thickness is negligible compared to other dimensions), the lateral dimensions can be considered infinite. In this case, a two-dimensional model of conduction is considered "a cylindrical propagation of field lines in the thin layer" and gives [12]:

$$\frac{U}{I} = K \frac{\rho}{t} \quad (I.12)$$

With: ρ : the resistivity of the layer.

t: thickness.

K: coefficient ($K = \frac{\ln 2}{\pi}$).

The report $\frac{\rho}{t}$ characterizing the layer is noted R_s and is expressed in Ω .

At an available K coefficient, R_s is the ratio between the voltage U and the current I. According to the preceding observations, we have the formula to deduce the resistivity of the four-point measurement knowing the thickness[12]:

$$\rho = \left(\frac{\pi \cdot U}{\ln 2 \cdot I} \right) \cdot t = R_s \cdot t \quad (I.13)$$

And their conductivity is:

$$\sigma = \frac{1}{\rho} \quad (I.14)$$

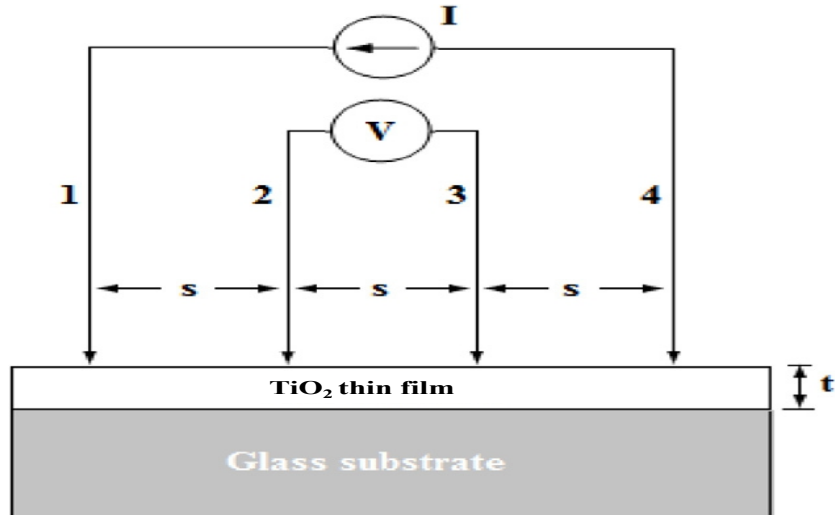


Figure.I.22 Schematic diagram of the Four-Point Probe used to determine the electrical resistivity of the TiO₂ thin film , on a glass substrate[39].

Chapter II :

Generalities about titanium dioxide TiO_2 .

In this chapter we are presented a brief survey on structural, optical and electrical properties of TiO₂ thin films and their most important applications in various technological areas.

II.1 Titanium dioxide

Titanium is one of the most common elements on earth.(Its percentage in the earth's crust is about 0.63%)[\[1\]](#), the usual form of titanium in nature is metal oxide and not pure metal.and its usual oxide is Titanium dioxide[\[2\]](#).

Titanium dioxide [titanium(iv) oxide or titania] is an inorganic substance has a molecular formula TiO₂ with 79.87 as molecular weight[\[3\]](#).

TiO₂, a non-toxic material, chemically stable, that is nonflammable, and not hazardous. It is an n-type metal oxide semiconducting material, biocompatible and strong oxidizing agent (with large surface area) has very high photocatalytic activity. It is an inexpensive material with high dielectric constant and low production cost[\[4\]](#).

II.2 Properties of TiO₂

II.2.1 Structural properties

Titanium dioxide is a compound with many polymorphs, and rutile (R), anatase (A) and brookite (B) are the most common crystal structures.A comparison of the properties of the three polymorphs is summarized in Table.[II.1](#).

II.2.1.1 Anatase

Anatase (tetragonal, space group I4₁/amd) crystal structure is constituted by distorted TiO₆ octahedral sites sharing four corners, and it has two low energy surfaces, (101) and (001), which are common for natural crystals. The (101) surface which is the most prevalent face for anatase nanocrystals[\[5\]](#).

Anatase is the most stable phase for nanoparticles below 11 nm, and its fundamental band gap is indirect, it was determined experimentally to be 3.2 eV with electrochemical measurements at room temperature (RT), anatase is the first phase to crystallise during the heat treatment of amorphous TiO₂ [6].

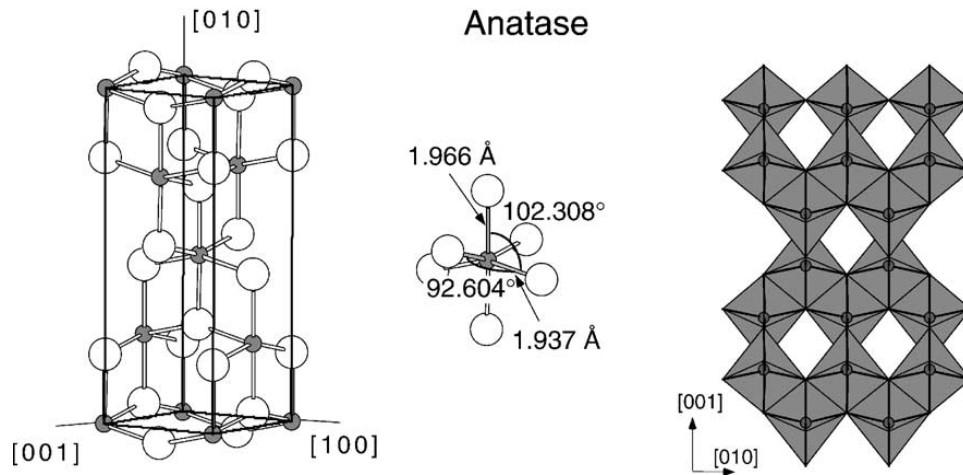


Figure II.1 Structure of anatase [7].

II.2.1.2 Brookite

The brookite phase, which is rarer and more difficult to prepare. The structure of brookite (orthorhombic, space group Pbc₂a, the structure with lower symmetry among the counter-polymorphs), is also made by distorted octahedral sites elongated along c-axis and each octahedron shares three edges with adjacent octahedra, and the order of stability of the crystal faces is $.010/ < .110/ < .100/$, brookite is the most stable phase for nanoparticles in the 11-35 nm range [5].

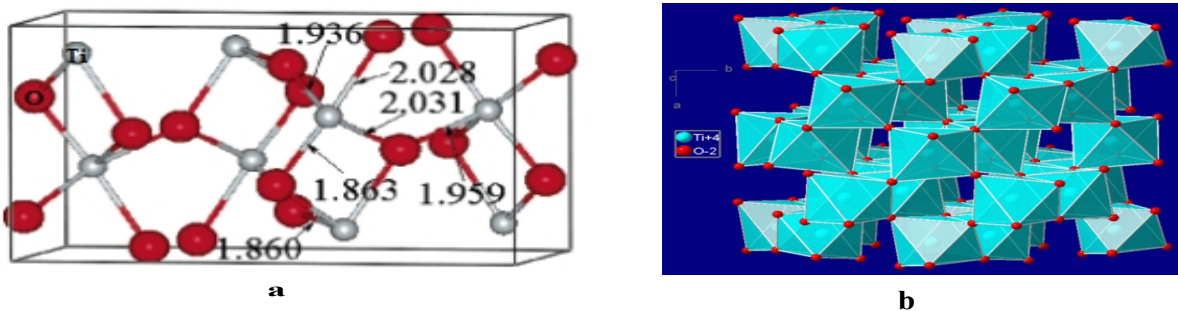


Figure II.2 (a) Structure of the brookite phase of TiO₂, (b) the arrangement of the constitutive octahedron of brookite [8,9].

II.2.1.3 Rutile

The structure of rutile (tetragonal, space group $P4_1/mnm$) is made by chains of TiO₆ octahedra that share a vertex along c-axis. Rutile has three main crystal faces, two that are quite low in energy and are thus considered to be important for practical polycrystalline or powder materials, these are: (110), (001) and (100), the most thermally stable is (110).

The rutile phase is stable at most temperatures and pressures up to 60 kba, and the (001) face is thermally less stable [10], and it is the most stable phase for particles above 35 nm in size [5].

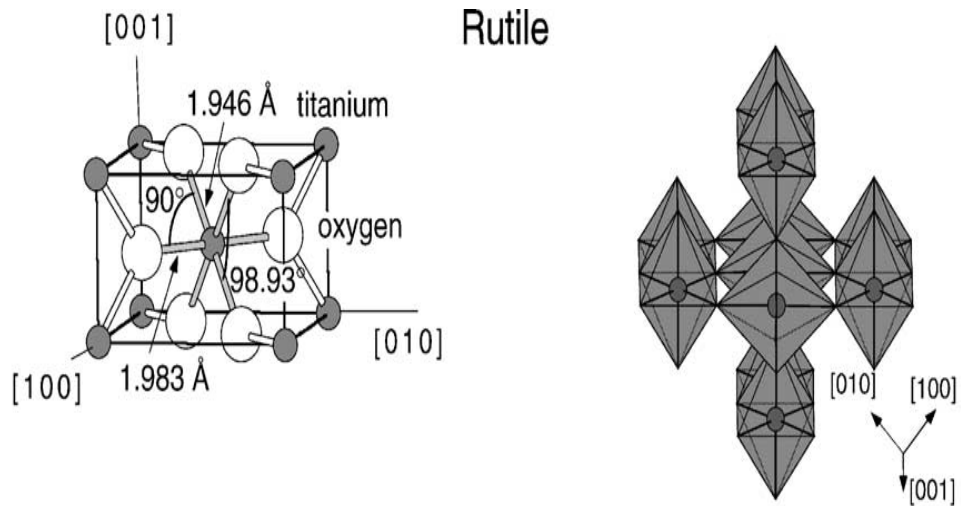


Figure.II.3 Structure of rutile [7].

Table.II.1 Comparison of the rutile, anatase, and brookite, different crystal structures of TiO₂[11],[12],[13],[14].

Phase	Anatase	Rutile	Brookite
Structure and space group	Tetragonal I 4 ₁ /amd	Tetragonal P 4 ₂ /mnm	Orthorhombic Pbca
Lattice parameter (Å) (T = 350°C)	a = b=3.7923 c = 9.5548	a =b= 4.5930 c = 2.9590	a = 5.4558 b = 9.1819 c = 5.142
Molecule/cell	4	2	8
Density (g.cm ⁻³)	3.84	4.26	4.12
Ti-O bond length (Å)	1.937(4) 1.965(2)	1.949(4) 1.980(2)	1.87~2.04
O-Ti-O bond angle	77.7° 92.6°	81.2° 90.0°	81.2°~90.0°
Band gap (eV)	Direct 3.42 indirect 3.46	Direct 3.04 indirect 3.05	3.14
Refractive index λ = 600 (nm)	2.48 - 2.55	2.60 - 2.89	2.57-2.69
Dielectric constant	31-48	89-173	78
Electron mobility (10 ⁻⁴ m ² /V.s)	Crystal: 15–550 Thin film: 0.1–4	Crystal: 0.1–10 Thin film: 0.1	---
Nature of conductivity at room temperature	n-type semiconductor	n-type semiconductor	---

In comparison with other polymorphs, anatase-TiO₂ is preferable for solar-cell applications because of its high electron mobility, low dielectric constant, and lower density. Anatase-TiO₂ also has a slightly higher Fermi level, a lower capacity to adsorb oxygen, and a higher degree of hydroxylation compared with other phases. These properties increase the

photoactivity of TiO₂. Based on charge-carrier dynamics, chemical properties, and activity of photocatalytic degradation of organic compounds, anatase-TiO₂ appears to be the most active photocatalytic polymorph.

II.2.1.4 Stability of TiO₂ phases

TiO₂ thin films are generally amorphous for deposition temperatures $\leq 350^{\circ}\text{C}$, above which anatase is formed. The most stable crystalline phase, rutile, is formed at temperatures greater than about 600°C .

The metastable anatase and brookite phases can irreversibly convert to stable rutile upon heating .

The phase transformation brookite \rightarrow rutile occurs in the thermal range of $500 - 700^{\circ}\text{C}$, whilst anatase transforms into rutile from 600 to 1100°C .

The anatase-to-rutile (A \rightarrow R) phase transformation – exothermal and irreversible – follows a nucleation-growth mechanism . Upon heating, anatase crystallites increase their size till they reach a critical dimension (r_c) and the A \rightarrow R transformation begins . The polymorphic reaction occurs through a cooperative movement of Ti and O atoms after the breaking of anatase Ti – O bonds.

The temperature of the A \rightarrow R phase transformation is affected by several factors, such as: crystallite dimension, grain size , atmosphere or the presence of dopants.

As anatase or brookite transforms to rutile, significant grain growth takes place, resulting in lower surface area. This is one of the reasons why rutile often exhibits poorer photocatalytic performance in comparison with the metastable anatase and brookite phases[13].

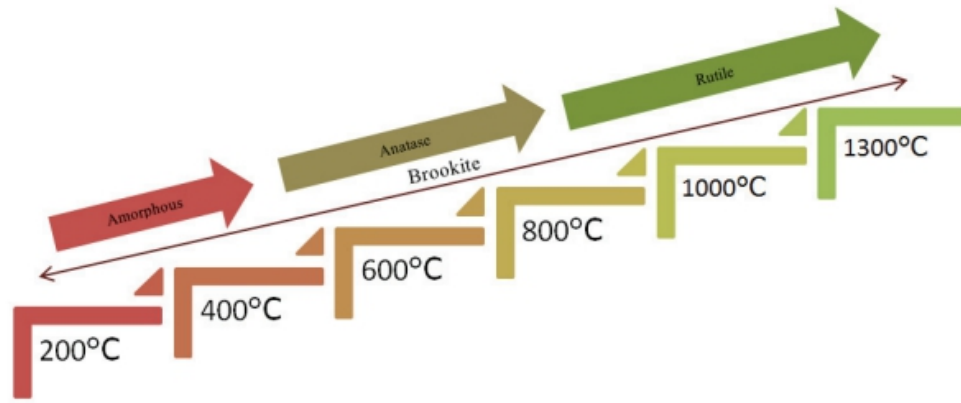


Figure.II.4 Phase transition of titanium dioxide[15].

II.2.2 Optical properties

TiO₂ is presented as a semiconductor material with a wide band-gap. This wide band gaps enable the reflection of visible light. Yet, anatase is capable of reflecting a wider electromagnetic wave constituting of long-wave ultraviolet light(UVA)beside the visible[3].

The transparency of TiO₂ in the visible, associated with an absorption edge around 0.42 μm leads to a strong absorption in the ultraviolet, which gives it excellent properties, such as protection against UV radiation [16].

The different varieties of titanium oxide have a high refractive index n in the visible range. Among the three stable crystalline phases, rutile has the highest index ($n \sim 2.7$ at 500 nm), higher than that of the anatase variety ($n \sim 2.3$ at 550 nm)[17], This combined with a diffusion coefficient of the high visible light[16].

II.2.3 Electrical properties

TiO₂ is a semiconductor. It is characterized by a gap ranging from 3 to 3.2 eV between the top of the valence band and the bottom of the conduction band. Classically, when TiO₂ is excited by a photon of energy equal or higher than the value of its bandgap, an electron “jumps” from the valence band to the conduction band and creates a hole in the valence band (**Figure.II.5**). This photogenerated electron-hole pair (so-called exciton) can promote redox reactions. This effect has been called Honda-Fujishima effect, from the names of the first two scientists who discovered it in 1972[18].

The energetic levels of the valence band are mainly made up of the 2p orbitals of the oxygen atoms, the energetic levels of the conduction band are made up of the 3d orbitals of the titanium atoms [18].

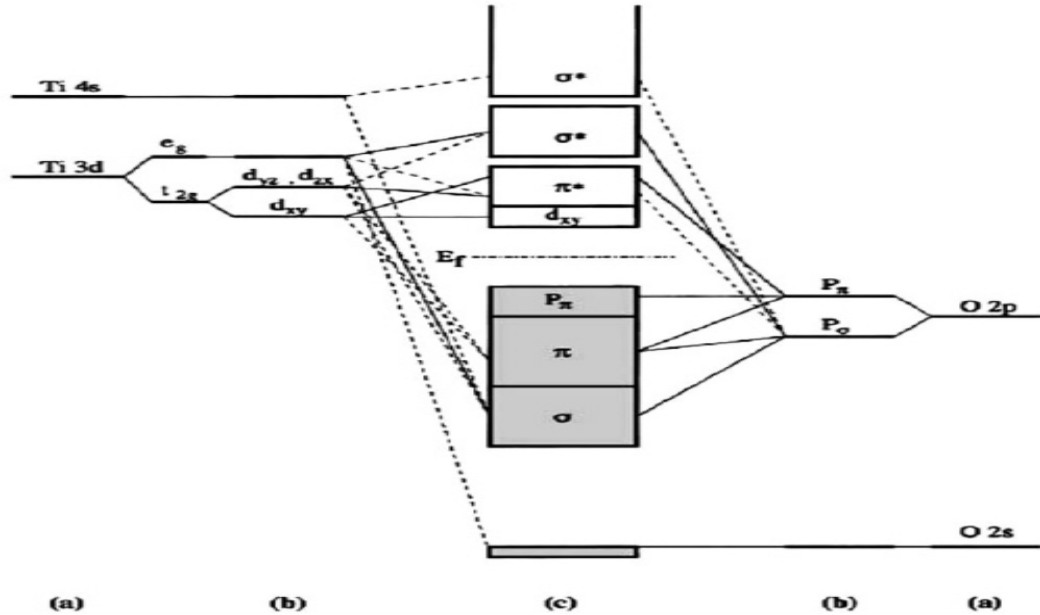


Figure.II.5 Molecular-orbital bonding structure for anatase TiO₂: (a) atomic levels, (b) crystal-field split levels, (c) final interaction states. The thin-solid and dashed lines represent large and small contributions, respectively [19].

II.2.4 Photocatalytic properties

The basic mechanism of TiO₂ photocatalysis is as follows: UV irradiation induces the formation of electron-hole pairs, whose charge carriers react with chemical species such as water molecule and molecular oxygen in the air to produce hydroxyl radicals ($\cdot\text{OH}$) and superoxide radical anions ($\text{O}_2^{\cdot-}$), respectively, which contribute decomposition of organic molecules at the TiO₂ surface (**Figure.II.6**). These oxidation processes can be used to environmental cleaning for air and water purification [20].

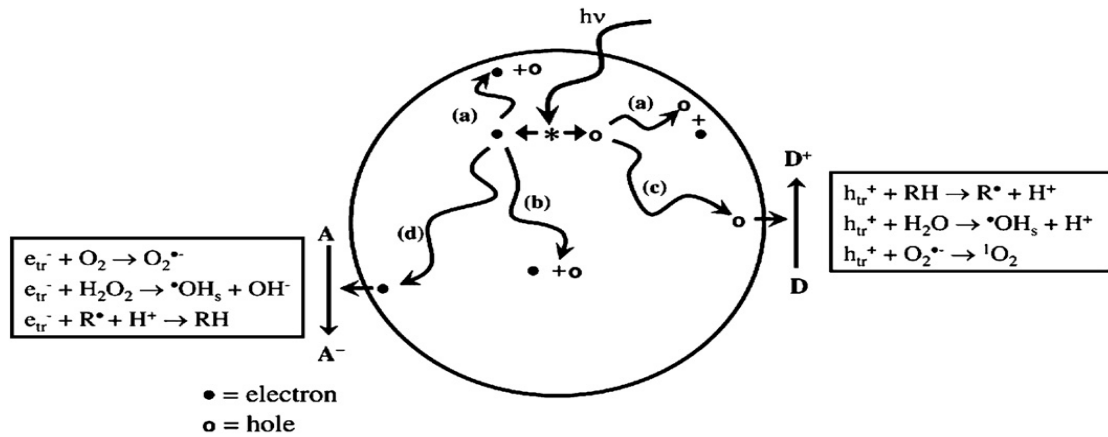


Figure.II.6 Processes occurring on bare TiO₂ particles after UV excitation[5].

In addition, TiO₂ surfaces become highly hydrophilic under UV light irradiation (**Figure.II.7**). The mechanism involves photogenerated holes produced in the bulk of TiO₂ trapping at lattice oxygen site. Trapped holes may break the bond between lattice titanium and oxygen ions and water molecules coordinates titanium sites.

The water molecules release a proton for charge compensation, and then a new OH group forms, increasing the number of OH groups at the surface. The coordinated new OH groups have high surface energy, which afford highly hydrophilic surface[20].

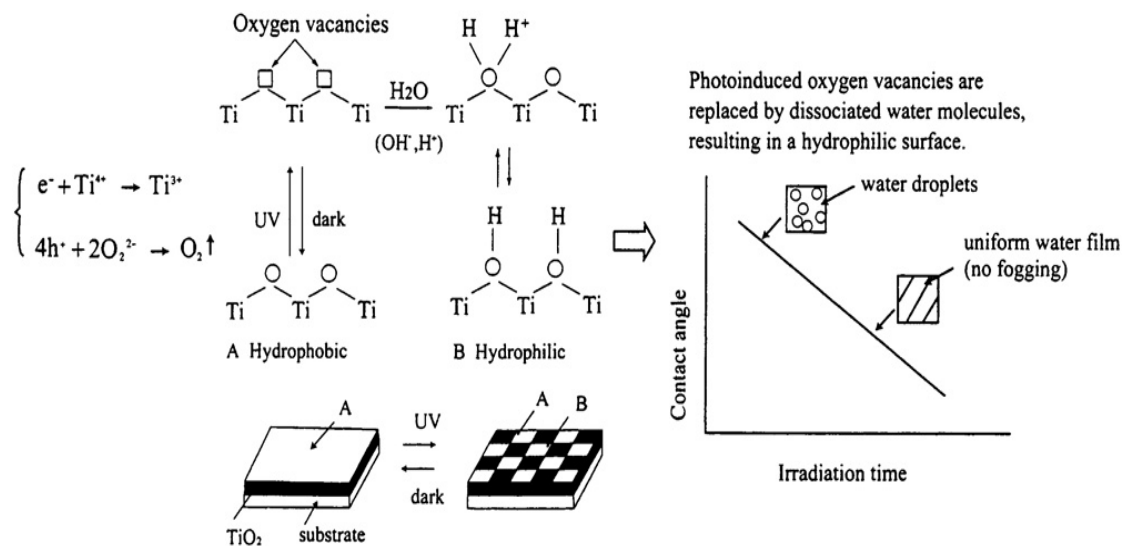


Figure.II.7 Mechanism of photo-induced hydrophilicity [21].

II.3 Importance and applications of TiO₂ thin films

Titania has advantageous properties such as chemical stability, non-toxicity, and low cost, so it has received a great deal of attention. Titania has a very high refractive index (~2.4) and

low visible absorptivity. It is favored in the field of coatings and in thin film optical devices, and also has the wide band gap (~3.2 eV) that can be exploited in the field of optical coatings combined with the high ultraviolet absorption. Wide band gap materials have the advantages of being able to operate at higher temperatures and having a longer carrier lifetime, reducing recombination losses. It also has an interesting property of self-cleaning where it prevents growth of bacteria and fungi when exposed to sunlight, meaning buildings, which are constantly exposed to sunlight, can be protected by coated with a thin layer. This is because the absorption range of TiO₂ is in the UV range of the solar spectrum that prevents any damage caused by UV light[11].

TiO₂ is used in wastewater purification, inorganic membranes[22], and as catalyst supports. Titanium oxide is also being used in heterogeneous catalysis, as a photocatalyst, in solar cells for the production of hydrogen and electric energy [23],[24]. Titania has excellent biocompatibility with respect to bone implants, and also finds applications in nanostructured form in Li-based batteries and electrochromic devices [25]. These uses can be generally classified into "energy" and "environmental" types.(As demonstrated in Figure. II.8).

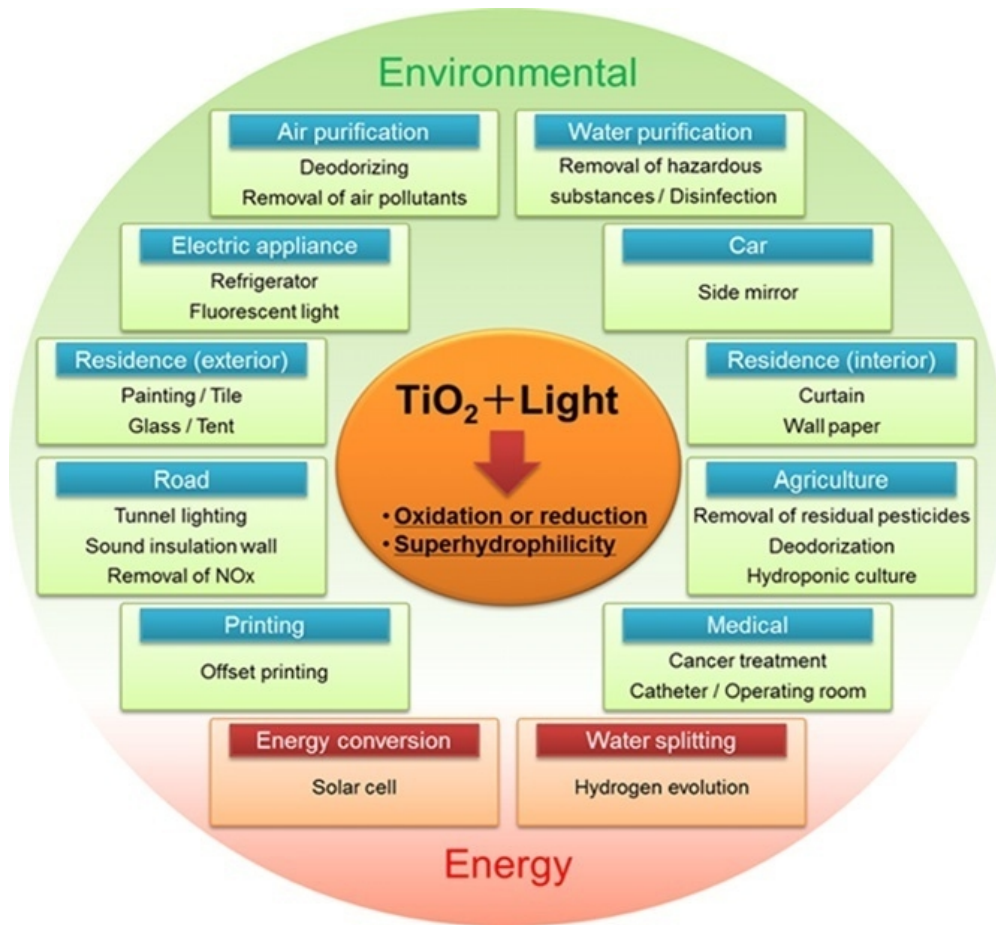


Figure. II .8 Applications of TiO_2 [26].

Chapter III :

Experimental procedures, results and discussions.

This chapter describes the experimental procedures for developing thin films by the sol gel route using the spin coating technique, in addition to describing the results of different characterization techniques (X-ray diffraction, UV-Visible spectroscopy, scanning electron microscope and Four-point probe method), which allowed us to make a detailed study of the structural, optical, morphological, chemical and electrical properties .

III.1 Detailed experimental condition

III.1.1 Used apparatus (spin coater)

The spin coater which was used to deposit the TiO₂ thin films has the following shape (Figure.III.1).



Figure.III.1 Spin coating.

III.1.2 Materials used

For the preparation of films, titanium (IV) isopropoxide (Ti [OC-H (CH₃)₂]₄) used as a precursor of TiO₂ , were used. Further, stabilizer agent acetyl acetone (CH₃COCH) also the organic solvents such as, methoxyethanol (C₃H₈O₂), ethylene glycol(C₂H₆O₂),methanol (CH₃OH), ethanol (C₂H₅OH) and isopropanol (C₃H₈O) were used to prepare the precursor solution.

III.1.2.1 Properties of the materials used

We present the different physico-chemical properties of the elements used in the deposition :

Precursor (Titanium (IV) isopropoxide)

-Synonym: Titanium (IV) isopropoxide.

-Appearance: Colorless to light yellow liquid.

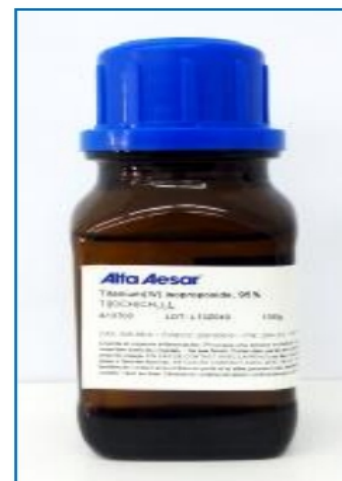
-Molar mass: 284.23 g / mol.

- Density: 0.955 g / cm³.

- Purity: 95%.

-Solubility: Soluble in alcohol.

-Boiling temperature: 232 °C.



Stabilizer agent (Acetylacetone)

-Formula: C₅H₈O₂.

-Appearance: Transparent liquid.

-Molar mass: 100.12 g / mol.

-Density: 0.97 g / cm³ at 20 °C.

-Purity: 99.5%.

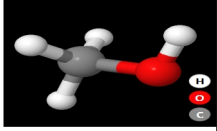
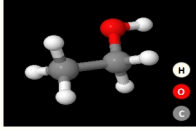
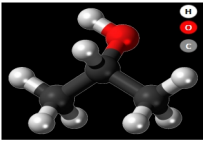
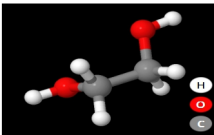
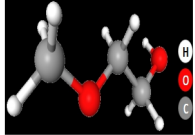
-Boiling point: 140.4 °C.



Solvents (ethanol ,methanol , isopropanol,methoxyethanol and ethylene glycol)

The properties of the solvents used in the deposition are shown in the table. **III.1.**

Table.III.1 The properties of the solvents.

Solvent	Methanol	Ethanol	Isopropanol	Ethylene glycol	Methoxyethanol
Structure and molecular weight (g/mol)	CH ₃ OH 32.04 	CH ₃ CH ₂ OH 46.07 	(CH ₃) ₂ COH 60.10 	HOCH ₂ CH ₂ OH 62.07 	CH ₃ OCH ₂ CH ₂ OH 76.10 
Boiling point (°C)	64.7	78.3	82.3	197.3	124-125
Melting point (°C)	-97.7	-114.1	-88	-12.3	-85
Density (g/ml)	0.7866	0.7851	0.7810	1.1097	0.965
Solubility in 100g of water	Miscible	Miscible	Miscible	Miscible	Miscible
Solubility of water in 100g of solvent	Miscible	Miscible	Miscible	Miscible	Miscible
Dielectric constant	32.6	24.55	19.9	37.7	16.90
Dipole moment	1.6	1.7	1.66	2.2	2.04
Viscosity (10 ⁻³ Pa · s) at 25 °C	0.5445	1.078	2.073	16.13	1.7
Surface tension (10 ⁻³ J/m ²)	22.1	22	18.3	47	31.80

III.1.2.2 Why we used of these alcohol solvents ?

We have selected these different alcohol solvents (methanol, ethanol, isopropanol and ethylene glycol) for these following reasons:

- ✚ They all has lower boiling points in comparing to TTIP i.e. easy to separate out.
- ✚ Due to the similarities of the -OR groups in the TTIP with -OR' groups in the alcohol solvent, in order to the best control of both hydrolysis and gelation.
- ✚ TTIP are not miscible in water.
- ✚ In view of the difference in their properties (carbon numbers, boiling points, viscosity and dielectric constant).

III.1.3 Preparation of TiO₂ thin films

III.1.3.1 Solution preparation

The key steps for sol–gel solution preparation are as follows:

Firstly starting material, 0.2M of titanium (IV) isopropoxid (TTIP) was separately dissolved in various solvents namely: methoxyethanol (C₃H₈O₂), ethylene glycol (C₂H₆O₂), methanol (CH₃OH), ethanol (C₂H₅OH) and isopropanol (C₃H₈O). Secondly, the solution contained beaker was placed on the magnetic stirrer. Thirdly the stabilizing agent, acetyl acetone (AcAc) (CH₃COCH) solution was adding drop by drop until titanium (IV) isopropoxide (Ti [OC-H (CH₃)₂]₄) and (AcAc) reach a molar ratio of 1:1. The resultant solution was continuously stirred at 50°C for 3 h to allow hydrolysis and condensation reactions to occur. Finally, we get the aged sol–gel solution, and it is used for coating process.

III.1.3.2 Preparation of the substrate

a) Choice of substrat

During this study, TiO₂ thin films were deposited on glass substrate (see **Figure.III.2**). Which have a 2.5cm ×2.5cm surface area, the choice of glass for these reasons:

- The thermal compatibility with TiO₂ (thermal dilation coefficients is $\alpha_{glass} = 3.3 \times 10^{-6}K^{-1}$, $\alpha_{TiO_2} = (8 - 10) \times 10^{-6}K^{-1}$) which minimize the stress in the interface film/substrate.

- For their transparency which adapts well for the optical characterization of films in the visible one.
- For economic reasons.
- In order to obtain good adherence and uniformity for the films.



Figure.III.2 Glass substrates.

b) Cleaning of the substrate

The cleaning of the surface of the substrate is a very important issue in thin film deposition technology. The exposure of the substrate surface to the atmosphere generates gaseous, liquid or solid contaminations which should be removed before the deposition process. When the substrates are not clean, the deposited film usually does not adhere well and the desired film properties are affected by the impurities on the surface of the substrate, thus the cleaning of the substrate is one of the most important steps.

The cleaning of our substrates surfaces is as follows:

- Rinsing with the water distilled and then with acetone during 5 min.
- Rinsing with distilled water.
- Rinsing with ethanol during 5 min at ambient temperature.
- Cleaning in water distilled bath.
- Drying using a drier.

III.1.3.3 Depositing of thin films

The deposition procedure comes right after the preparation of the solution and the substrates.

The solution were spin coated on glass substrate using coating which is 4000 r.p.m. for 30 seconds. Each layer consists of drops of the solution and each sample was coated with 5 layer coating. Between every layer, the sample was preheated at 250°C for 10 minutes to evaporate the solvent and remove organic residuals. Finally, the sample was annealed at 600°C for 2 hour to remain its anatase phase. This same procedure was used to prepare all the TiO₂ thin films using five different solvents (**Figure.III.4**). The preparation of TiO₂ thin films is shown in **Figure.III.3**.

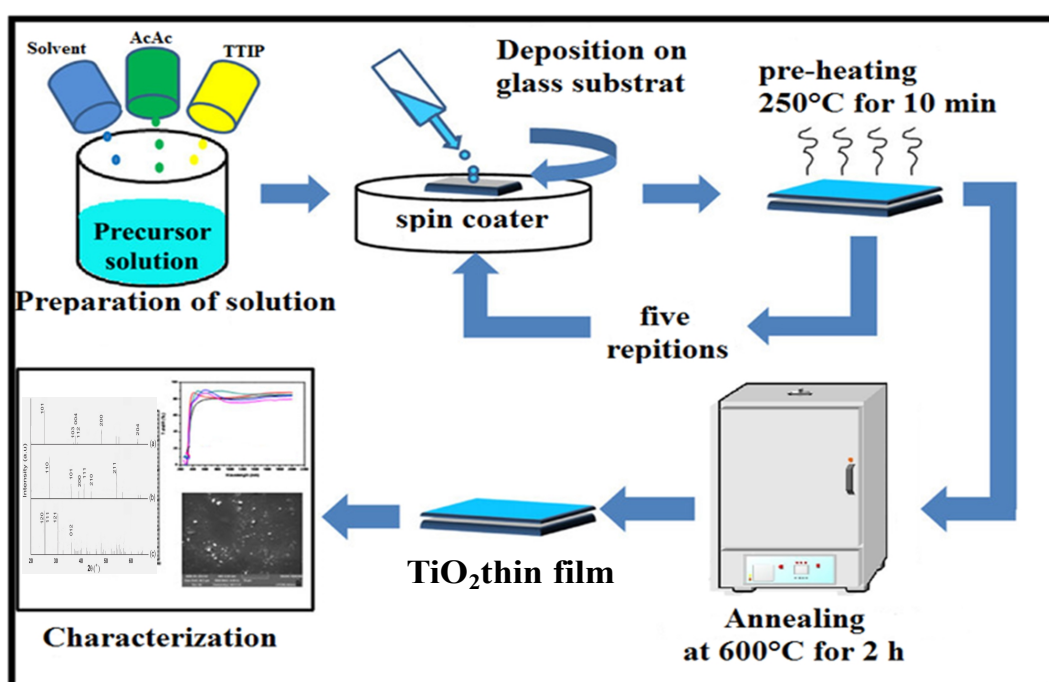


Figure.III.3 Schematic represents the experimental procedure.

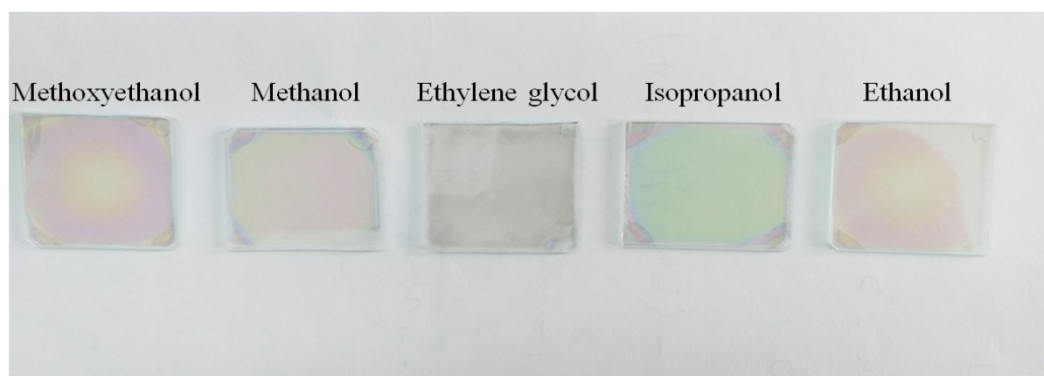


Figure.III.4 Photograph of our five films prepared with different solvents .

III.2 Results and discussions

In our calculations, we have followed methods mentioned in the second chapter.

III.2.1 Adhesion test

Adhesion is very important in thin film technology because the thin films (usually < 1 μm and in some applications of the order of 50 nm) are so fragile that these must be supported by more substantial substrates and the degree to which the film can share the strength of the substrate depends upon the adhesion between the two.

III.2.1.1 Simple test used

An adhesive tape is applied to the film surface and pulled off again(Figure.III.5).The tape test is a subjective test which is not only dependent on the type of tape but also on the pull off velocity and the pull off angle.

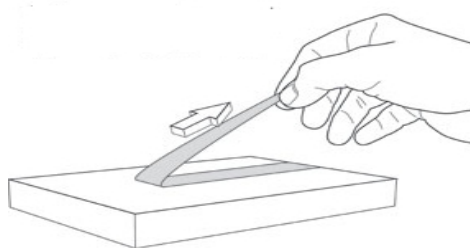


Figure.III.5 Simple test of adhesion.

III.2.2 The thickness of the film

Weight difference method can be used to measure thickness. You measure mass of the film before and after deposition. The difference will give you the mass of the film ($m[\text{g}]$). You know the area of the film ($A [\text{cm}^2]$) and density ($d [\text{g}/\text{cm}^3]$) of the film material. By using following relation you can find out thickness ($t [\text{cm}]$)[1]:

$$t = \frac{m}{A \times d}$$

The thickness values of our thin TiO_2 films are measured by interference fringe and different de mass methode presented (see the table.III.2).

Table.III.2 The thickness of TiO₂ thin films deposited using different solvents.

Solvents	t (nm)
Methanol	663.41
Ethanol	654.43
Isopropanol	384.55
Methoxyethanol	283.88
Ethylene glycol	147.12

We present the variations of the thickness of our films in the following Figure :

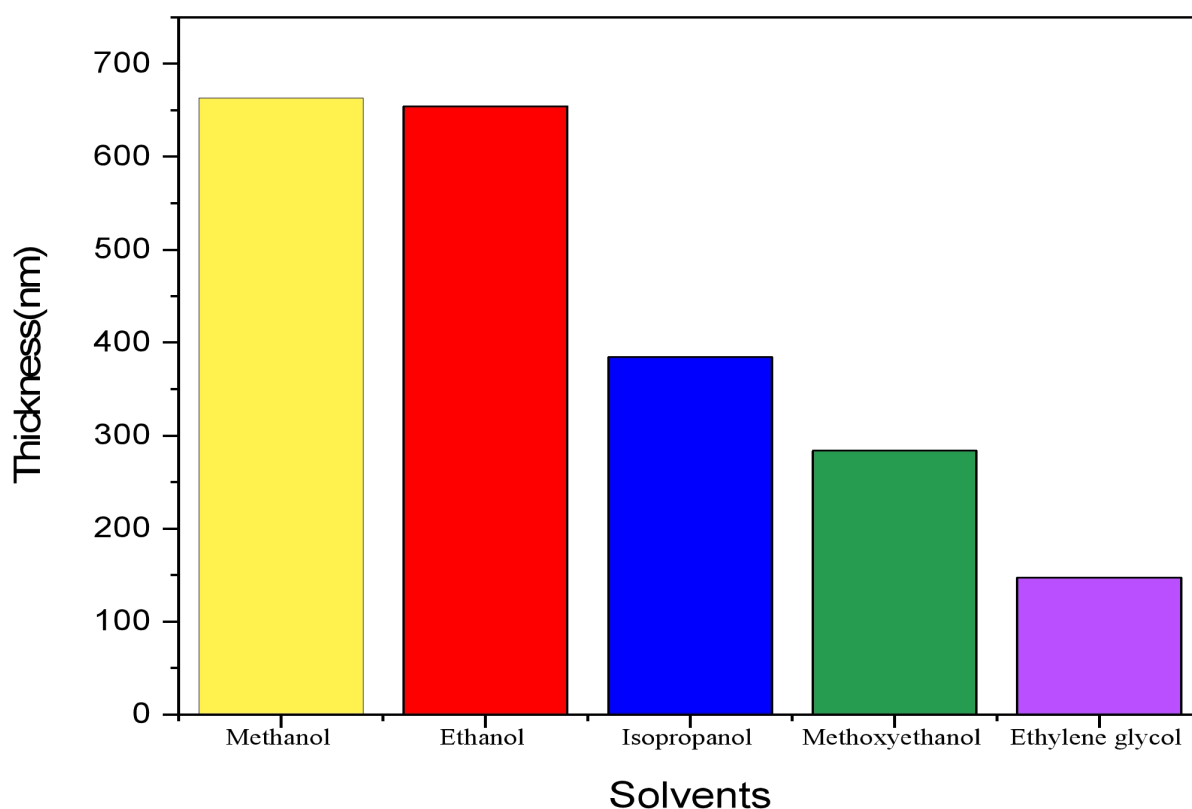
**Figure.III.6** The variations of the thickness as a function of solvents.

Figure.III.6 shows variations of the film thickness as a function of the used solvent . It is clear that the films thickness depends to the type of the solvents, its values are as follows: 663.41, 654.43, 384.55, 283.88 and 147.12 nm for the solvents, methanol,ethanol,isopropanol,methoxyethanol and ethylene glycol,respectively, this variation in thickness is due to the difference in boiling point of the solvent, this results in a difference in the activation energy his, (which is the minimum energy required for the reaction to

occur). Hence, depending on the solvent the rate of hydrolysis and gelation time of the solutions differs. Hence, there will be a difference in the polycondensation of the resulting titanium alkoxides $Ti(OR)_z$ affecting the thickness of the TiO_2 thin films, and this result can be observed clearer in Figure.III.7 [2-3].

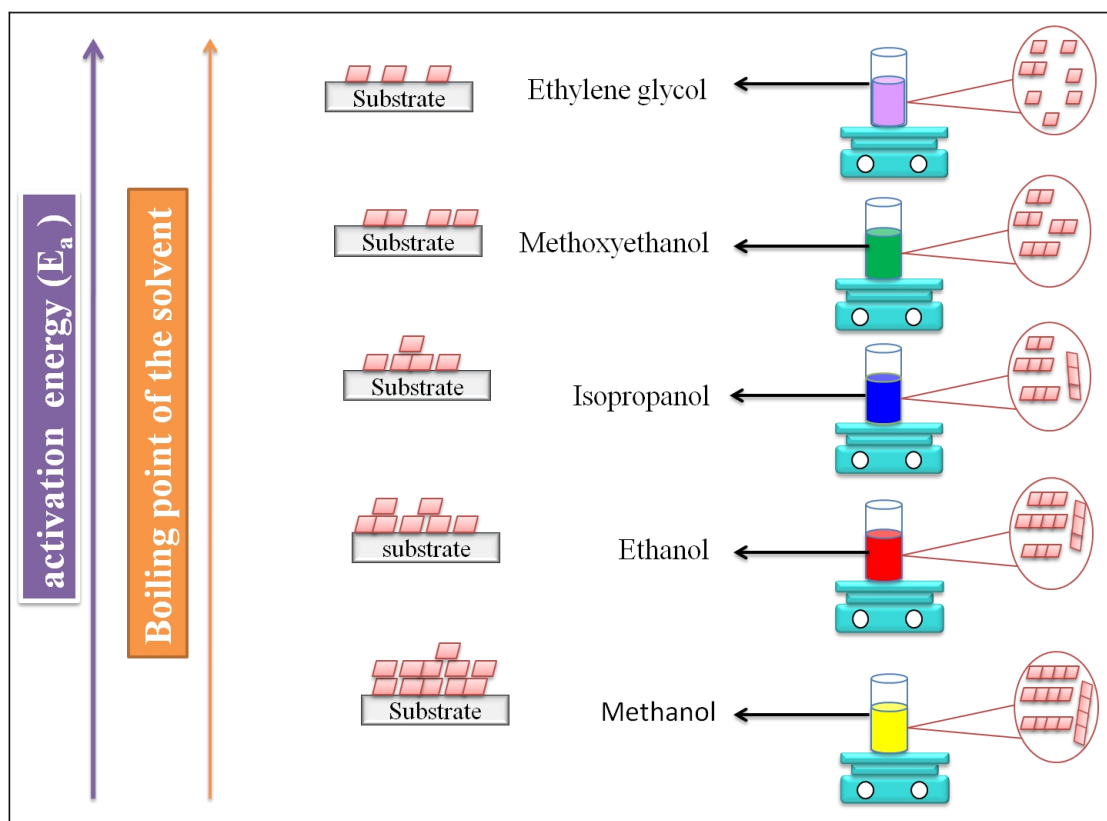


Figure.III.7 Schematic illustration of the impact of boiling point on titanium alkoxides $Ti(OR)_z$ distribution in solutions.

III.2.3 Structural characterization

X-ray diffraction studies highlight any internal regularity and in the case of TiO_2 will distinguish between the various forms (i.e., anatase, rutile, and brookite) or will reveal if the films are amorphous, grain size, the dislocation density. In order to determine the effect of different solvents under constant experimental conditions. The diffractometer used for the characterization of our samples is of the Mini-Flex type (RigaKu) with copper anode having an X-ray beam of wavelength $K\alpha(Cu) = 1.5418 \text{ \AA}$. Measurements were taken under beam acceleration conditions of 40 kV/35 mA. The angular domain (in 2θ) scanned is between 20° and 60° . This technique makes it possible to obtain the diffractograms shown in Figure.III.9. These diffractograms are compared using the ASTM files (JCPDS N ° 21-1272) for the anatase phase (**Figure.III.8**).

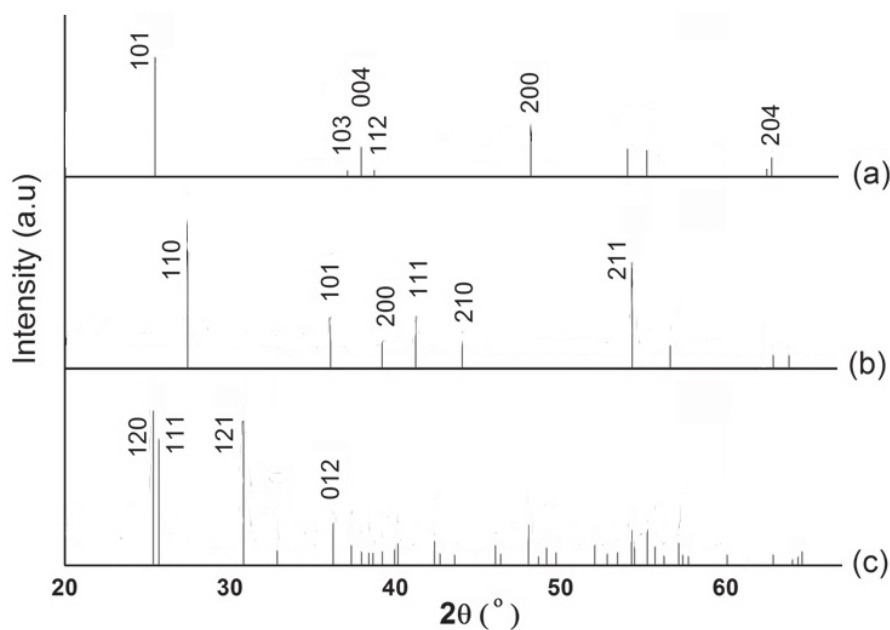


Figure.III.8 Reference sheets (JCPDS) specific to TiO_2 (a) anatase (JCPDS 21-1272), (b) rutile (JCPDS 21-1276) and (c) brookite (JCPDS 29-1360) [4].

We have reported in Figure.III.8 the spectra of X-ray diffraction of TiO_2 prepared in different solvents.

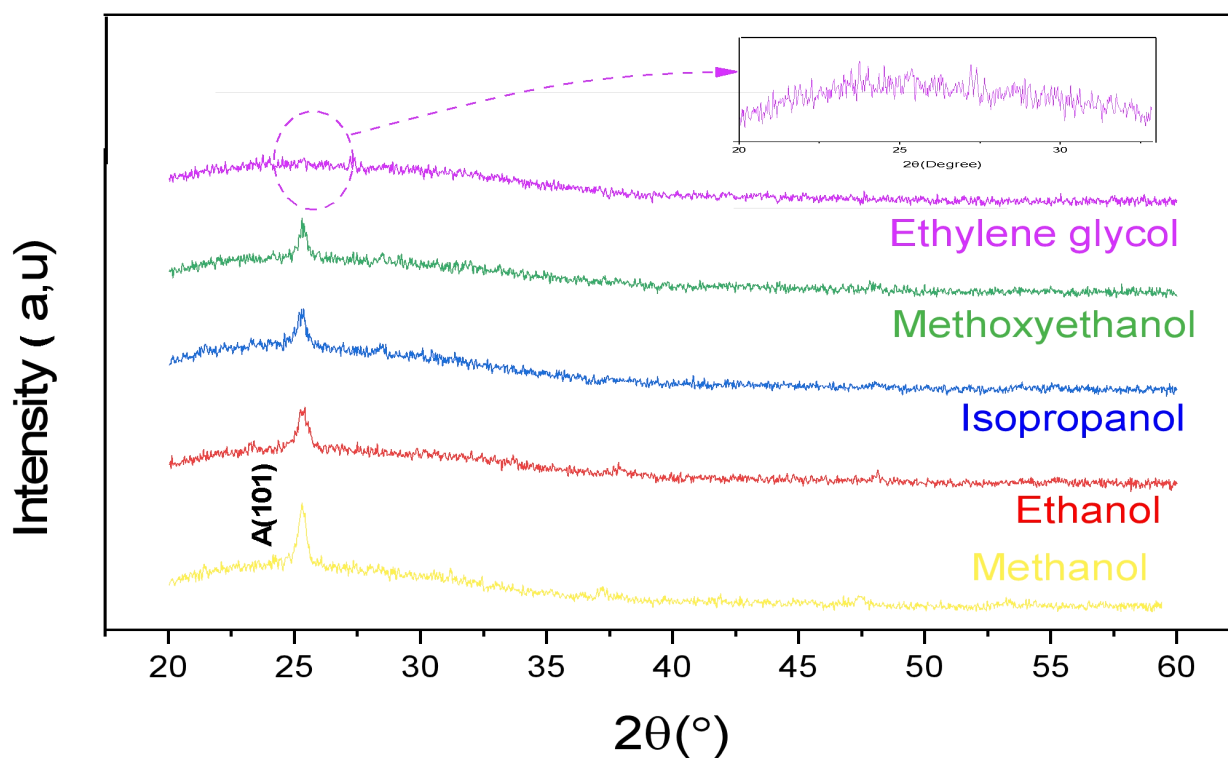


Figure.III. 9 X-ray diffraction patterns of TiO_2 thin films as a function of the used solvent.

From the comparison between the results obtained (**Figure.III.9**) and the ASTM sheet for TiO₂ (**Figure.III.8**). It can be seen that the diffraction pattern of TiO₂ thin film prepared in ethylene glycol solvent, does not exhibit a clear peak and especially the peak around 25.281° is absent which indicates that the films are amorphous. This is due to fewer nucleation sites (due to the large boiling point of the solvent).

While those films prepared from other solvents exhibited a clear diffraction peaks of anatase phase centered around 25.281°, the strong intensity of the peak indicates that the preferred orientation along (101) plane of all deposited films. This is due to the low surface energy of this plane in the anatase structure [5-7], also, regardless of the solvents used for preparing. The as-prepared films show that the main peak a slightly different (25.284°, 25.314°, 25.288° and 25.281° for methanol, ethanol, isopropanol and methoxyethanol, respectively), this variation caused by variation in defects of the films and alcohol solvents[8].

The intensity of the peaks about 370, 291, 301 and 284 for methanol, ethanol, isopropanol and methoxyethanol, respectively, it can be seen that the intensity of the peak is very higher for film prepared from methanol than other. This result is may be due to the increase in proportion of titanium oxide and the density of layer[9], the intensity of main peak is also different, caused by the difference in crystalline degree and crystallite size. Upon changing of alcohol solvents in sequence of increasing Dipole moment (methanol = 1.6, ethanol = 1.7, isopropanol = 1.66 and methoxyethanol = 2.04), the films became to lessen the crystalline degree, and the film produced in methanol is the best crystal. It can be clearly understood that the (methanol solvent) film exhibits a higher crystalline quality when compared with, other solvents.

No peaks corresponding to the rutile or brookite phase were observed in the X-ray diffraction pattern in all the solvents.

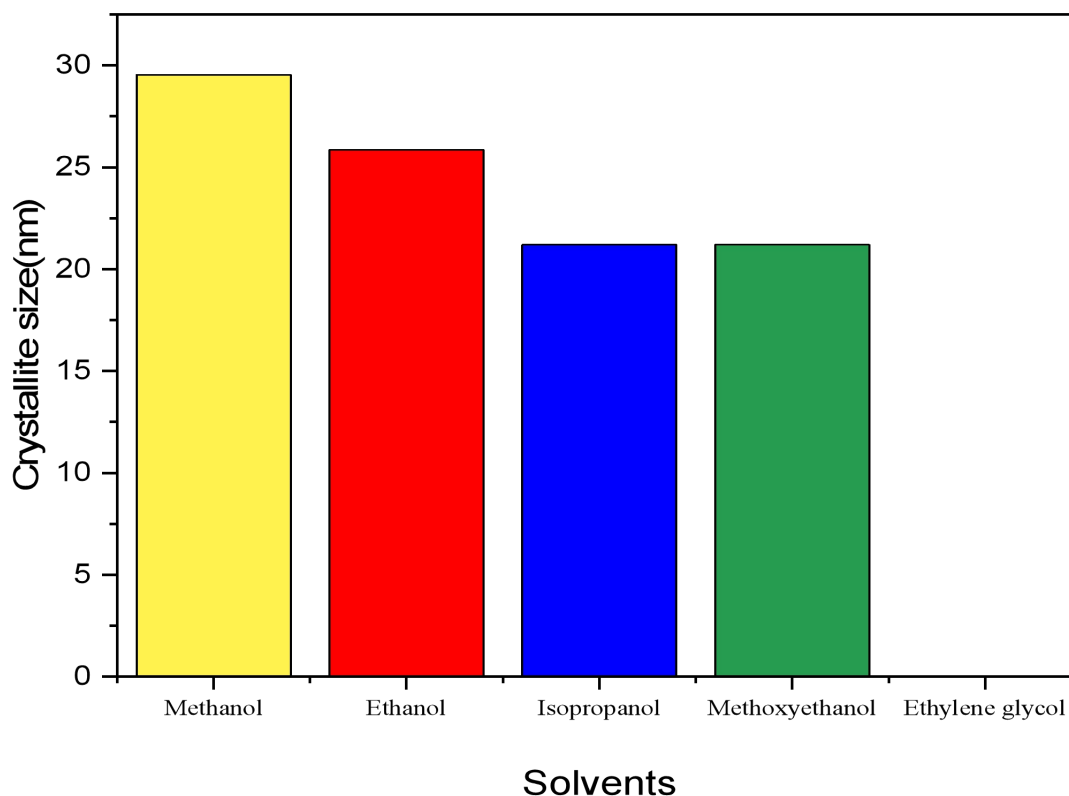
III.2.3.1 Crystallite size

The crystallite size of the various TiO₂ films were calculated from the highest peak, using the relation (I.2) and the results are shown in the table.III.3.

Table.III.3 The variation of crystallite size according to solvents .

Solvent	Crystallite size(nm)
Methanol	29.541
Ethanol	25.846
Isopropanol	21.194
Methoxyethanol	21.197
Ethylene glycol	-

Using these results we draw the variation of the crystallite size as a function of solvent which is represented in the Figure.III.10.

**Figure.III.10** The variations of crystallite size as a function of solvents.

All of the thin films prepared with various solvents (except film prepared with ethylene glycol solvent) attempted were generally identical but only showed different degrees of peak broadening due to the variation of crystallite sizes. Since the anatase crystals prepared with different solvents presented various sizes (shown in **Figure.III.10**), the crystalline size calculated according to the XRD peak of (101) face. The crystallite sizes (D_{101}) are 29.2, 25.8,

21.194, and 21.197 nm for methanol (CH_3OH , $(\eta) = 0.54 \cdot 10^{-3} \text{Pa}\cdot\text{s}$), ethanol ($\text{CH}_3\text{CH}_2\text{OH}$, $(\eta) = 1.07 \cdot 10^{-3} \text{Pa}\cdot\text{s}$), isopropanol ($(\text{CH}_3)_2\text{COH}$, $(\eta) = 2.07 \cdot 10^{-3} \text{Pa}\cdot\text{s}$) and methoxyethanol ($\text{CH}_3\text{OCH}_2\text{CH}_2\text{OH}$, $(\eta) = 1.72 \cdot 10^{-3} \text{Pa}\cdot\text{s}$), respectively. According to these results, the crystallite size seems to relate with viscosity (η) of the solvents. The solvents with a lower viscosity resulted in a Greater crystallite size than those with a higher viscosity. We also find that the crystallite size related to the carbon number and length of carbon chain of the solvent, when the comparison solvents, an increase in carbon number seemed to restrain the crystallization of anatase, which led to a smaller crystallite size [8-10].

III.2.3.2 The dislocation density and deformation

By exploiting the relation (I.3, I.4) (mentioned in chapter I), the deformation (ϵ) and the dislocation density (δ) of TiO_2 were determined. The results are grouped together in the following table.

Table. III .4 The Variation of dislocation density and deformation according to solvents.

Solvents	The dislocation density (nm^{-2})	Deformation
Methanol	0,00115	0,12
Ethanol	0,0015	0,128
Isopropanol	0,00223	0,141
Methoxyethanol	0,00223	0,141
Ethylene glycol	--	--

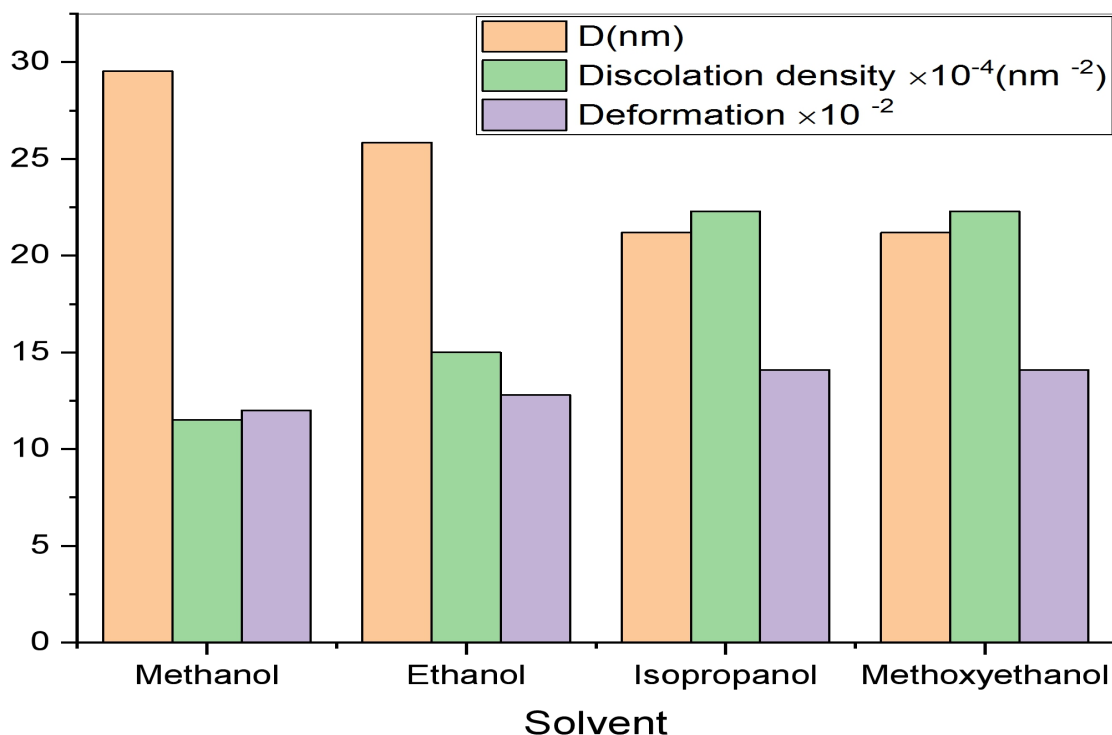


Figure.III.11 Structural parameters of TiO₂ thin films with different solvent .

Figure.III.11 and table.III.4 shows the variations of structural parameters such as crystallite size, dislocation density, and deformation. In general, good crystallization of the film had large crystallite size and small dislocation density and lower deformation values. Hence, the dislocation density and deformation values exhibit increases with the change in solvents from methanol to methoxyethanol, which indicates that methanol solvent has low crystal lattice imperfections. The reduction of lattice defects is due to decrease in strain and dislocation density.

III.2.4 The optical properties

The optical characterization of our thin films of TiO₂ has been done is obtained using a UV-visible spectrophotometer (Jasco V 770). The transmittance spectra of our samples are illustrated in the Figure.III.12:

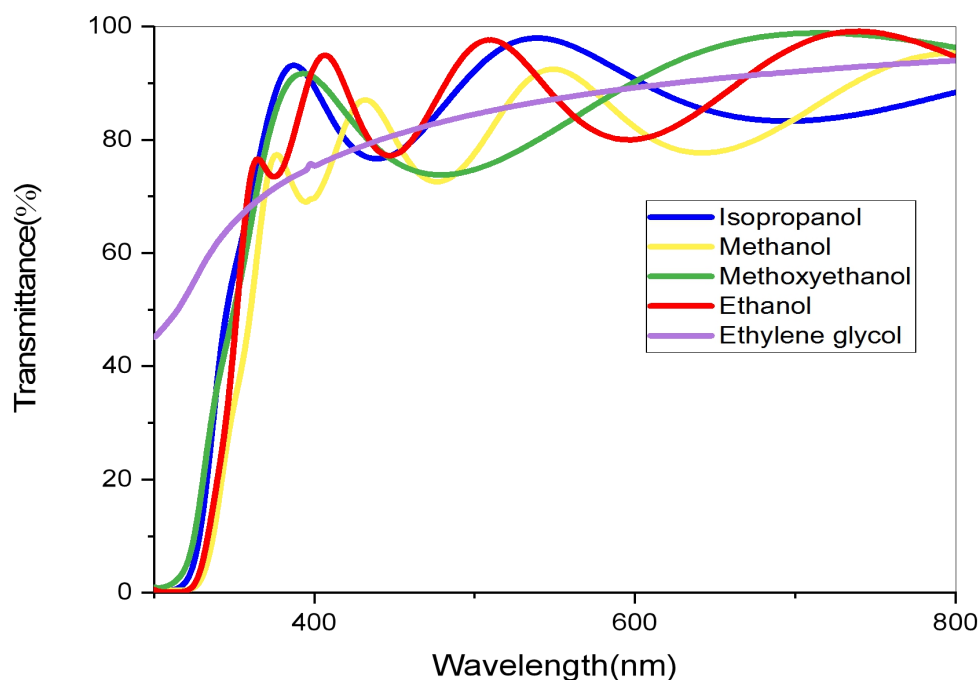


Figure.III.12 The transmittance spectra of TiO₂ films deposited using different solvents .

Figure.III.12 shows evolution of the optical transmittance spectra of the thin films of TiO₂ for various solvents, all the films obtained exhibit a higher transmittance reach to 90% in the visible region. All spectrums are characterized by the presence of two different regions:

(350 nm - 800 nm): the first region of high transparency showing a few interference oscillations which are due to multiple reflections at the film/substrate and the film/air interfaces .

($\lambda < 350$) : The second region corresponds to strong absorptions characterized by a sharp drop in optical transmission. This abrupt drop, which is the fundamental absorption of thin layers, is due to the electronic transition between the valence and conduction bands of semiconductor materials[9].

It has been observed that transmittance decreases with an increase in thickness, this is attributed to constructive interference, since the constructive and destructive interference is more obvious in thin films with a large thickness. In addition, since their thicknesses may vary, the effects of using different solvents cannot be compared [11] .

III.2.4.1 Optical Band gap energy

From the transmittance spectra, the direct and indirect optical gaps (E_g) were deduced for the TiO_2 films according to the method described in the previous chapter. and the results are shown in the table.III.5.

Table.III.5 direct and indirect band gap as various solvent for our films of TiO_2 .

Solvents	direct Bandgap (eV)	indirect Bandgap (eV)
Methanol	3,67	3,40
Ethanol	3,71	3,43
Isopropanol	3,73	3,46
Methoxyethanol	3,74	3,47
Ethylene glycol	3,52	3,35

Using these results we draw the variation of the band gaps indirect and direct as a function of solvent which is represented in the Figure.III.13 and Figure.III.14.

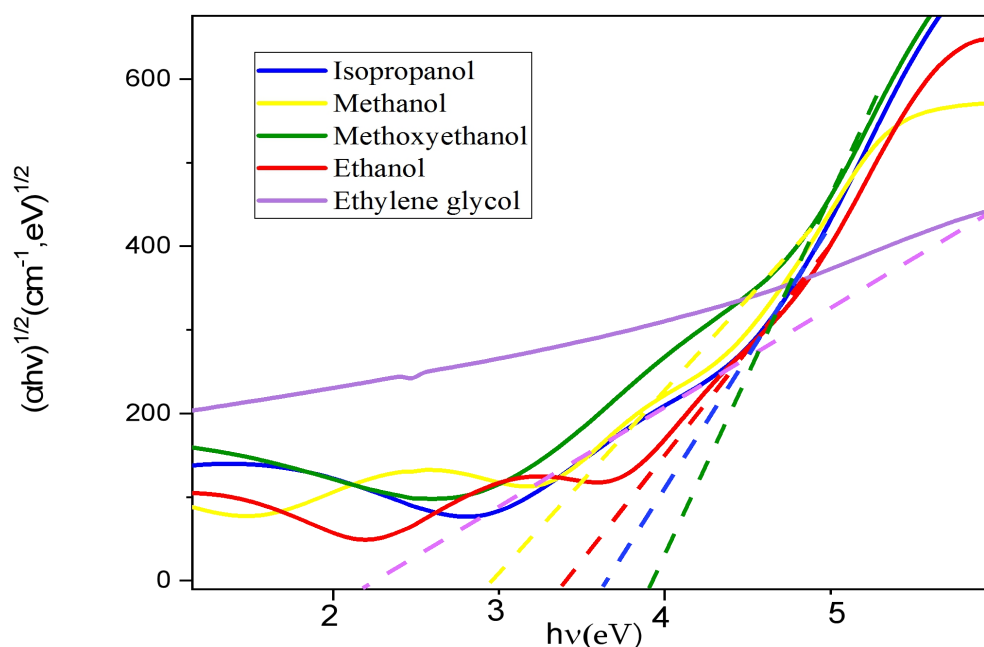


Figure.III.13 The Band gap indirect approximation using Tauc's plot.

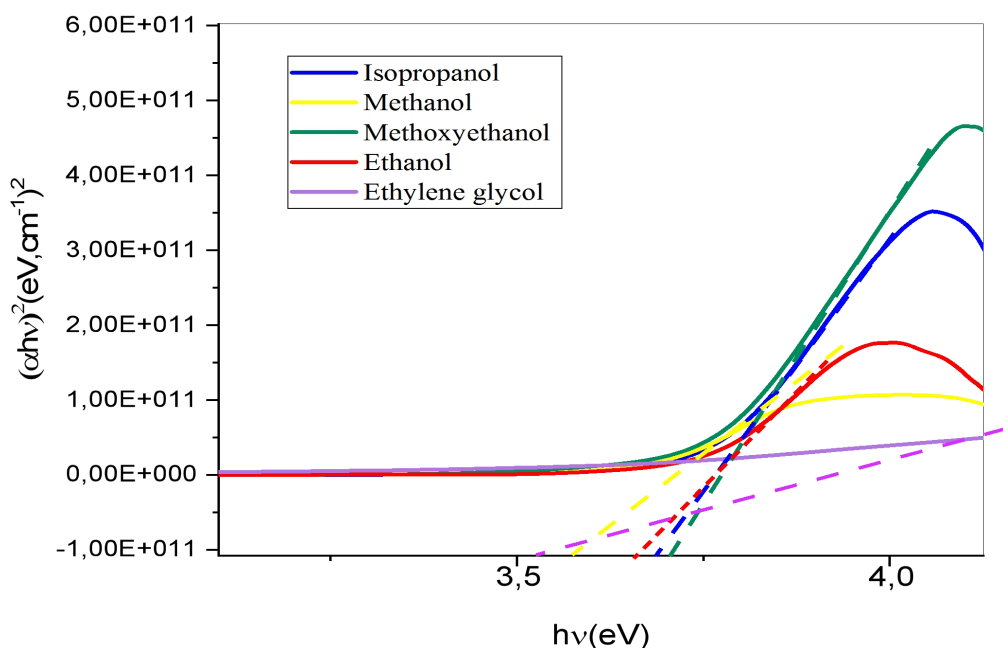


Figure.III.14 The band gap direct approximation using Tauc's plot.

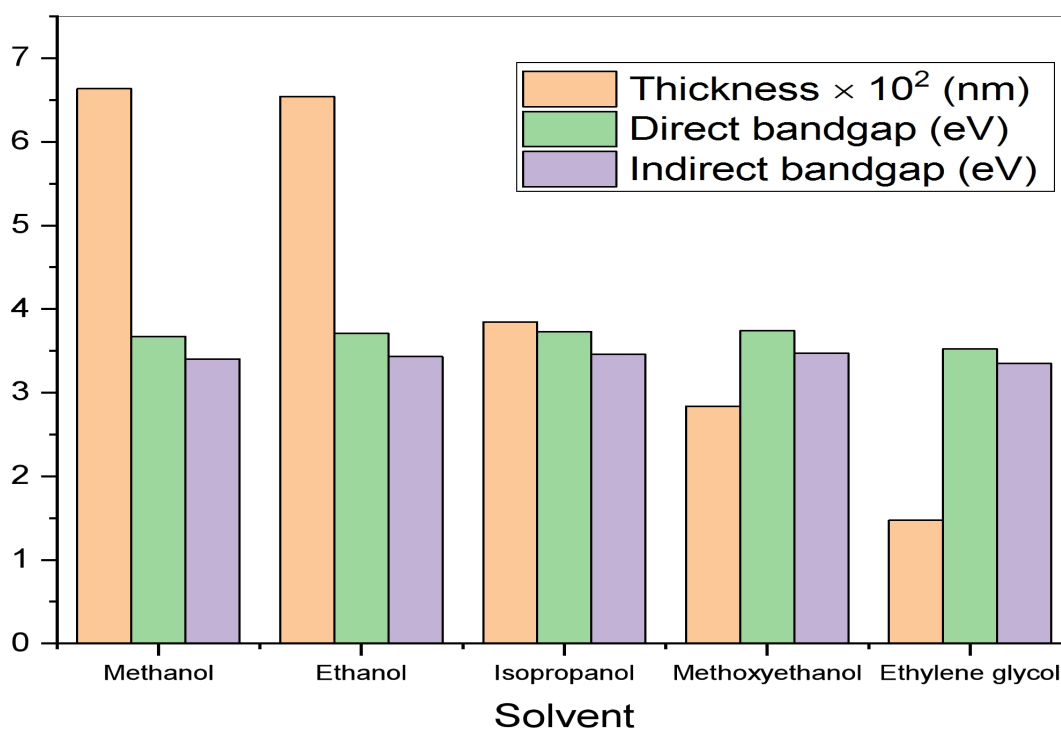


Figure.III.15 The variation of the optical gap energy (direct and indirect) and the thickness of TiO₂ thin films with different solvent.

As can be seen from Figure.III.15 and Table.III.5, the optical bandgap values decreased from 3.74 to 3.67 eV for direct allowed and from 3.47 to 3.34 eV for indirect allowed. with increasing film thickness. The decreasing in bandgap with increasing film thickness can be attributed to the improvement in the crystals, in morphological changes of the films, in changes of atomic distances and grain size and structural defects in the films. There is a

possibility of structural defects in the films due to their preparation at room temperature, this could give rise to the allowed states near the conduction band in the forbidden region. In case of thick films, these allowed states may as well merge with the conduction band resulting in the reduction of the bandgap[12]. But, this interpretation does not apply to ethylene glycol because it has an amorphous structure. Hence, the bandgap is small as possible due to the large number of crystal defects. This result is in agreement with literature and XRD results .

III.2.4.2 The Energy of urbach E_u (disorder)

The values of the disorder (E_u) are shown in the table.III.6 .

Table.III.6 Variation of the urbach energy as a function of the solvents .

Solvents	E_u (eV)
Methanol	0,16
Ethanol	0,15
Isopropanol	0,14
Methoxyethanol	0,13
Ethylene glycol	0,17

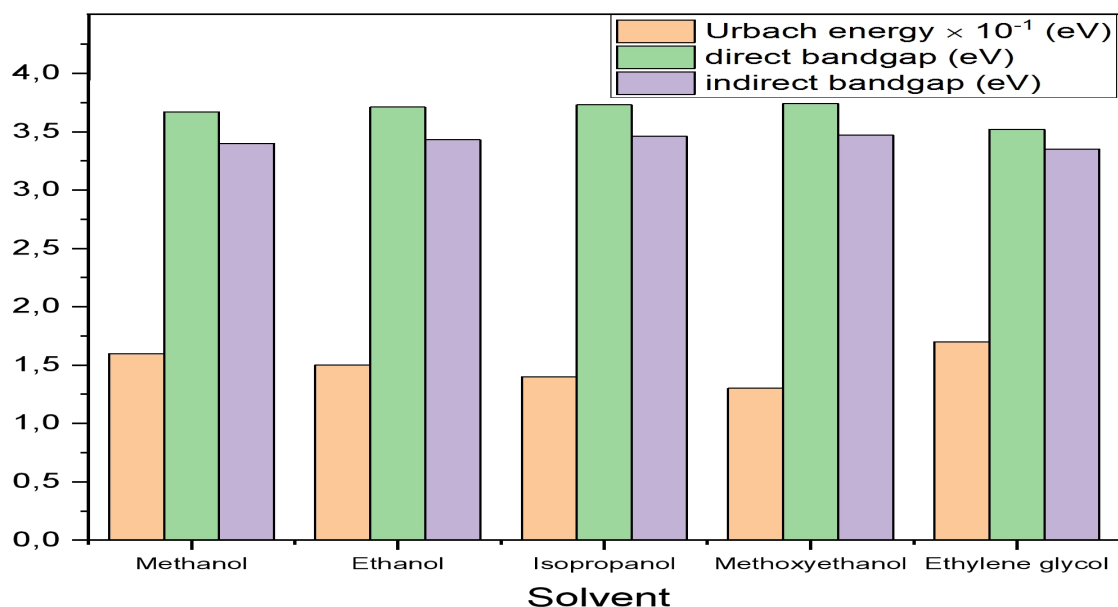
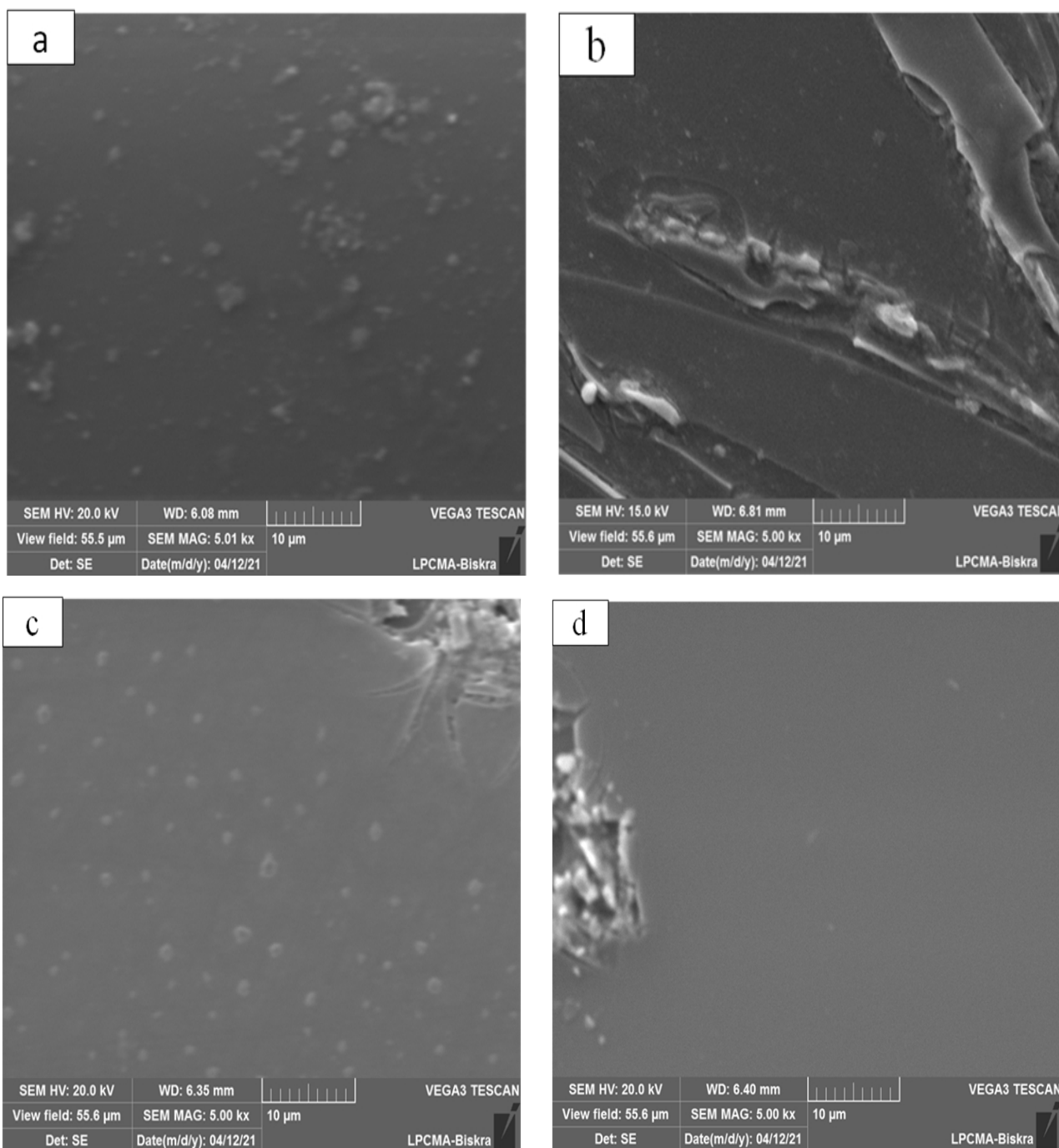


Figure.III.16 The variation of the optical gap energy (direct and indirect) and the Urbach energy of TiO_2 thin films with different solvent .

Figure.III.16 shows that there is variance in the energy of urbach (disorder) with difference Solvents. We can explain this phenomenon by the decrease in gap energy .

III.2.5 Surface Morphological Study

The surface morphology was studied by using the Scanning Electron Microscope, the SEM microstructure of the samples are given below :



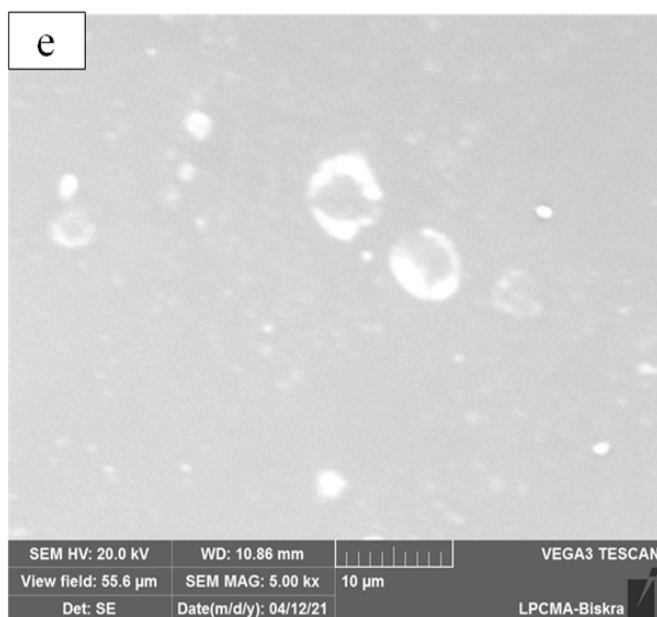
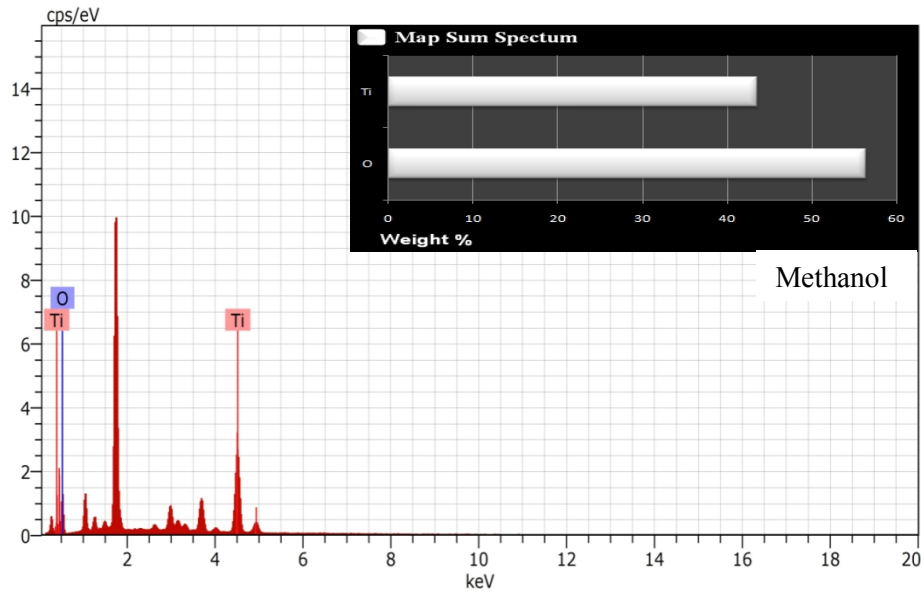


Figure. III.17 SEM images of TiO_2 thin films with different solvent .

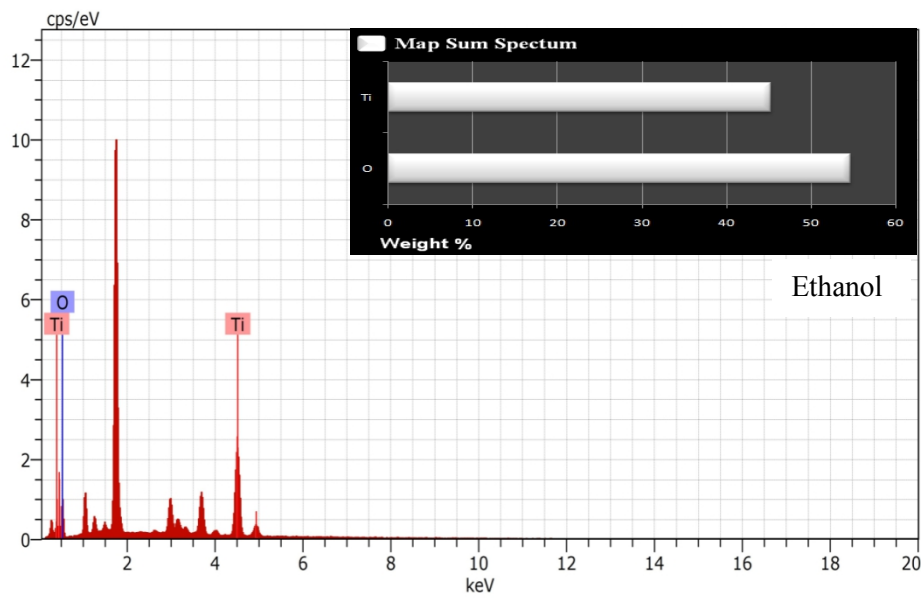
Figure.III.17 a–e shows the MEB images of Spin coated TiO_2 thin films with various solvents methanol, mthanol, isopropanol, methoxyethanol and ethylene glycol, respectively. The surface morphology of the films was found to be strongly dependent on the solven.

III.2.6 Chemical Properties

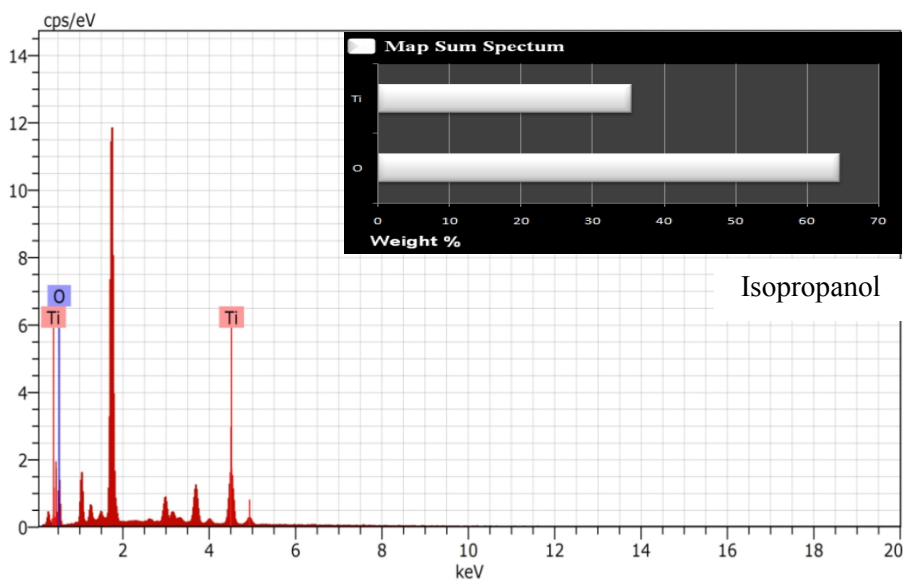
To assessment of the chemical composition of TiO_2 thin films with different solvents the energy X-ray dispersive spectroscopy (EDS) was done and the result is shown in Figure.III.18.



Methanol



Ethanol



Isopropanol

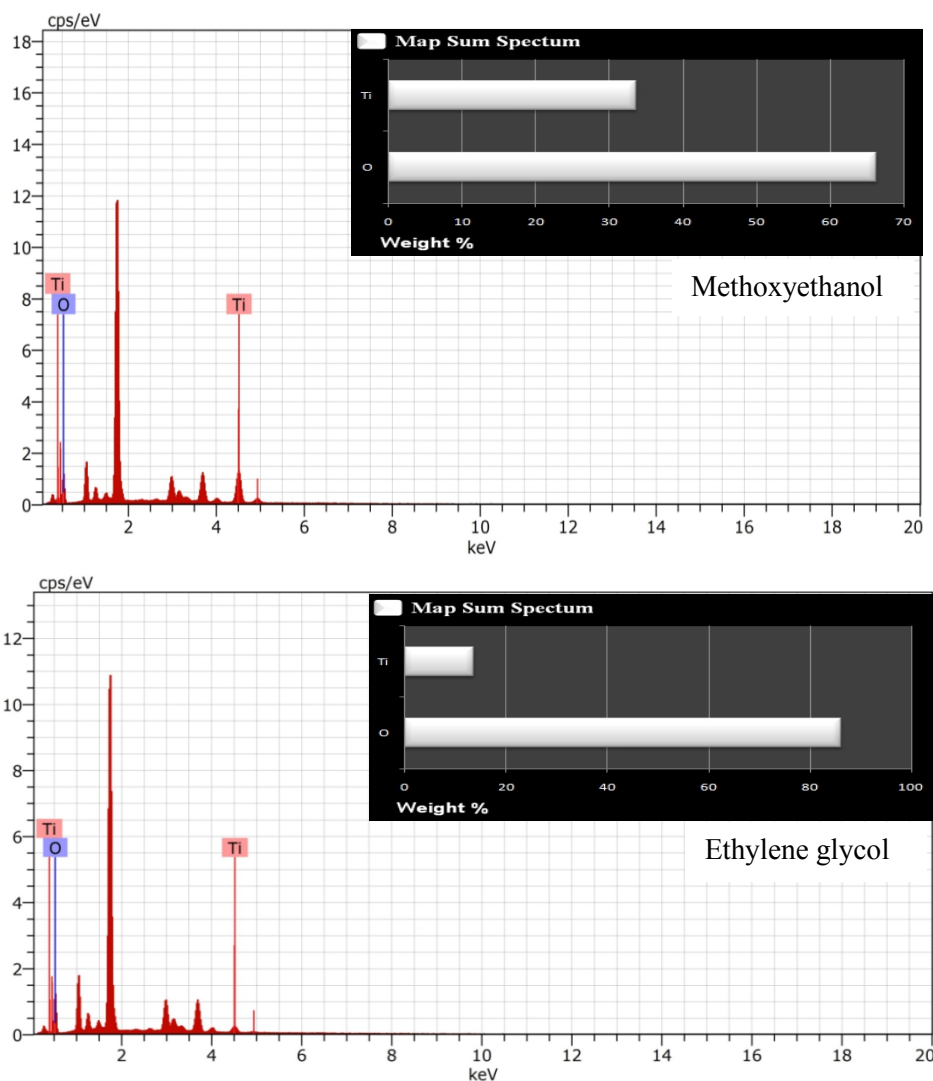


Figure. III.18 Energy dispersive spectra of TiO_2 prepared with different solvent.

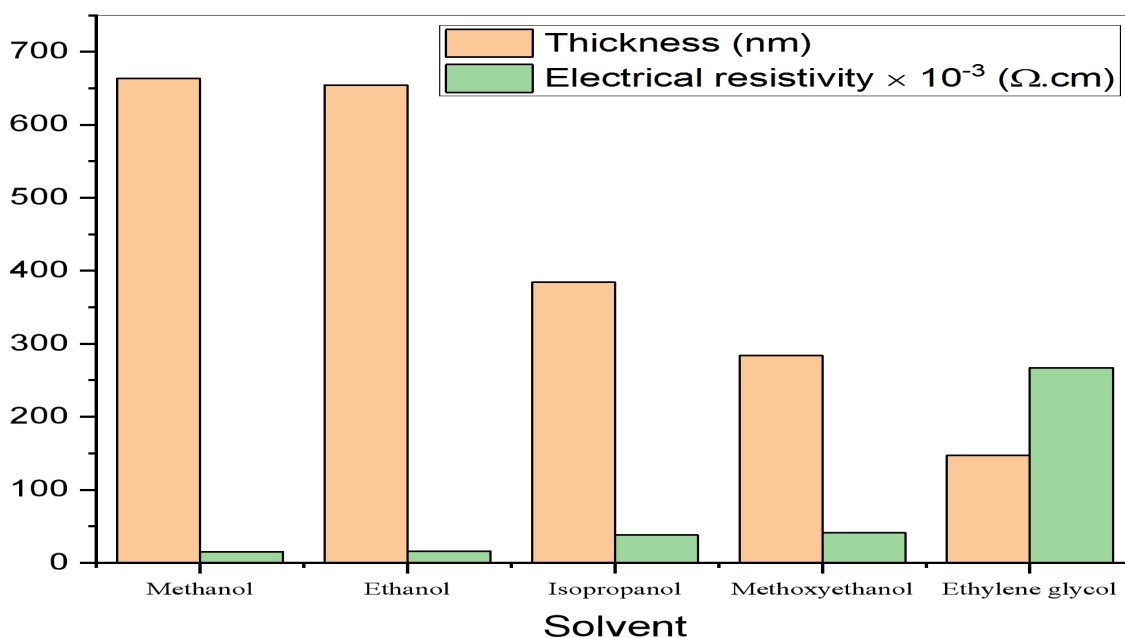
Figure.III.18 shows the EDS spectrum of TiO_2 thin films with different solvents, and it confirmed the presence of titanium oxide. From the EDS exhibits the presence of all core elements i.e. Ti and O .

III.2.7 Electrical Properties

For the determination of the conductivity and resistivity of Prepared with different solvents TiO_2 films, we use the Four-point method using the relation (II.13, II.14) and the obtained results are shown in Table.III.7:

Table.III.7 Resistivity and conductivity of Prepared with different solvents TiO₂ films.

Solvent	Electrical Resistivity(ρ) ($\Omega.cm$)	Electrical Conductivity(σ) ($\Omega.cm$) ⁻¹
Methanol	0.015	66,66
Ethanol	0.016	62,5
Isopropanol	0.038	26,31
Methoxyethanol	0.041	24,39
Ethylene glycol	0.267	0,0037

**Figure. III.19** The variation of the resistivity and thickness of prepared with different solvents TiO₂ films.

The results show (**Figure.III.19**) that the resistivity of the film decreases with increase in thickness of the film. The decrease in resistivity of the film is attributed to increase in cross-sectional area and rearrangement and removal of defects[13,14]. and Also, because the mean free path of the charged carriers is reduced, mainly due to scattering form impurities, at grain boundaries, and at the external surface(rough surfaces) [15].

We can also say ,since the TiO₂ is an n-type semiconductor materials, the existing concentration of Ti⁴⁺ in TiO₂ films forms a donor level between the band gap of TiO₂ which reduced the recombination rate of photo-generated electron–hole pairs. As a result, Ti⁴⁺ ion

have greater concentration in the films Prepared with high solubility solvents, which eventually caused an increase in the free electrons concentrations and subsequently caused reduction in films resistivity[16].

General conclusion

The work presented in this memory focused on the elaboration and characterization of thin films of TiO₂ Prepared with different solvents obtained by sol-gel (spin-coating).

TiO₂ thin films were prepared on glass substrates by sol-gel Spin coating technique using different solvents of methanol, ethanol, isopropanol, methoxyethanol, and ethylene glycol and Titanium Isopropoxide as precursor and acetylacetonone as stabilizer. The prepared films were characterised by XRD diffraction for structural properties, UV-Visible for optical characterization , SEM for morphology and finally the Four-point technique for determining electrical conductivity. The results obtained showed that:

- ✚ The solubility of titanium isopropoxide increases as the decreasing boiling point of alcohol solvents .
- ✚ The different alcohol solvents have the influence on the morphology and crystalline degree. In additional, the crystallite size of TiO₂ Films were found to be controlled by different alcohol solvents related to the number of carbon in alcohol and viscosity. The solvents with a lower viscosity resulted in a largest crystallite size than those with a higher viscosity. Moreover, an increase in carbon number seemed to restrain the crystallization of anatase, which led to a smaller crystallite size, the DRX results showed that the average crystallite size of all the samples was in the range of 21-29 nm.
- ✚ A shift in the optical band gap energy and electrical resistivity of the films from 3.74 to 3.35 eV and 0.267 to 0.015 Ω.cm, respectively, as a function of the thickness, has been observed. In addition, since their thicknesses may vary, the effects of using different solvents cannot be compared.

From our point of view, in order to study the effect of solvents on these properties, we give per solution own gel-forming time, depending on the solvent. Which allows us to study the effect of solvents better.

References Introduction General and Chapitre I

- [1]: A. Jilani et al, «modern technologies for creating the thin-film systems and coatings»,published by intech,2017,p.138-142.
- [2]:A.K.M. Muaz, «effect of annealing temperatures on the morphology, optical and electrical properties of TiO₂ thin films synthesized by the sol-gel method and deposited on Al/TiO₂/SiO₂/p-Si»,Microsystem Technologies Vol 22(4),2016, p 871-881.
- [3]:A. Mahyar,« Influence of solvent type on the characteristics and photocatalytic activity of TiO₂ nanoparticles prepared by the sol –gel method»,Micro & Nano Letters, 2011, Vol 6(4), p.244 –248.
- [4]:H.Frey,«Thin-Film Technology»,published by Springer-Verlag(Berlin Heidelberg), 2015, p. 1.
- [5]:L. Eckertová,«Physics of Thin Films»,published by Springer(US) , 1977,p. 115.
- [6]:K. Shin et al,«High quality graphene-semiconducting oxide hetero-structure for inverted organic photovoltaics», Journal Materials Chemistry Vol 22(26),2012,p.13032-13038.
- [7]:A. Barth,« Magnetic and structural properties of the Gd/Ni-Bilayer-System»,doctorat thesis, Universit at Konstanz Fachbereich Physik, 2015.
- [8]:Y. Zheng et al ,« Ultrathin Ferroelectric Films: Growth, Characterization, Physics and Applications» , journal materials Vol 7 ,2014,p.6377-6485.
- [9]:M. Florescu,«State-of-the-Art method for detection of azides by ¹⁴N-NMR spectroscopy and human health risk assessment»,doctorat thesis,Transilvania University ,2016.
- [10]:I.Mecheter , «Physical Properties of sol-gel Copper Oxide (CuO) Thin Films; Sol concentration effect », memory of Master ,Mohamed Boudiaf University(M'sila), 2019.
- [11]:A. Tracey et al , « Dye sensitisation of Sol-gel derived titanium dioxide films»,doctorat thesis,Sheffield Hallam University (United Kingdom), 1997.
- [12]: N.Djehaiche , «Effect of Niobium doping on the properties of Titanium Dioxide (TiO₂) Thin films elaborated by sol-gel(Spin-coating)», memory of master ,Mohamed Khider University (Biskra),2019.
- [13]:D.Levy et al ,« The sol-gel Handbook: Synthesis, Charact-erization, and Applications»,published by Wiley-VCH,2015,p.3
- [14]:C. Saravanan,« Chemical Reactions in Inorganic Chemistry », published by IntechOpen, 2018,p.32-42.

- [15]:A.P. Periyasamy et al,« Progress in sol-gel Technology for the Coatings of Fabrics», journal materials vol 13 (8),2020,p. 2-35.
- [16]:R. Pardon et al,«Photochromic organic-inorganic hybrid materials», Chemical Society Reviews Vol 40 (2), 2011,p. 672-87.
- [17]:G. Valverde Aguilar, « sol-gel Method - Design and Synthesis of New Materials with Interesting Physical, Chemical and Biological Properties»,published by intechopen, 2018,p.1-45.
- [18]:K. Jones et al,« solvent selection and the control of Sol-Gel reactions », Materials Research Society Vol 180,1990, p. 271-280.
- [19]:A. C. Marques,« Sol-gel process: an overview gel process: an overview», Department of Materials Science and Engineering, Lehigh University, Bethlehem (USA),2007,p. 1-6.
- [20]:Tocalo Co ,Jan. 2013.
- [21]:S. Gattal ,« Synthèse et étude des propriétés physiques des couches minces de SnO₂ » ,memory of master,Université Larbi Tébessi (Tébessa) ,2016.
- [22]:M.D. Tyona,« A theoretical study on spin coating technique», Advances in Materials Research Vol 2(4),2013,p.195-208.
- [23]:S.Heeravathi,« Spin coating methods and applications -a review », Journal of Xi'an University of Architecture & Technology Vol 7(6), 2020,p. 234.
- [24]:N. Sahu,« Fundamental understanding and modeling of spin coating » ,Indian J. Phys. Vol 83 (4) , 2009,p.493-502 .
- [25]:D. Winarski, «Synthesis and characterization of transparent conductive zinc oxide thin films by sol-gel spin coating methode »,memory of master, University in partial fulfilment (United States),2015,p. 13.
- [26]:P.Wang, « Polymeric Thin Films: Preparation, Surface Modification and Morphology», thesis doctorat, Columbia University(United States),2004.
- [27]:I.Ruzybayev,«Nanostructured nitrogen and carbon cod-oped TiO₂ thin films:synthesis ,structural characterization and optoelectronic properties » , thesis doctorat, University of Delaware,2014.
- [28]:K.Bedoud et al,«L'effet Thermique sur les Couches Minces du TiO₂ Déposé par la Méthode de Pulvérisation Cathodique », Proceeding of Engineering and Technology – PET ,Vol 30 ,p.43-46
- [29]:R.Messemche ,«Elaboration and characterization of undoped and doped titanium dioxide thin layers by sol-gel (spin coating) for photocatalytic applications», doctorat thesis,University Mohamed Khider (Biskra),2021.

- [30]:M. B.Tahir et al, «Review of morphological, optical and structural characteristics of TiO₂ thin film prepared by sol-gel spin-coating technique», Indian Journal of Pure & Applied Physics Vol 55, 2017, p. 716-721.
- [31]:O.Benkhetta , «Effet de la concentration de la solution sur les propriétés des couches minces de dioxyde de titane déposées par spray pyrolyse ultrasonique», Mémoire de master , Université Med Khider- Biskra, 2019.
- [32]:Q.Deng, «Band gap tuning and structural engineering of TiO₂ for photocatalysis and solar cells »,thesis doctorat, University (England),2012.
- [33]:F. S. Rocha et al,« Experimental Methods in Chemical Engineering: Ultraviolet Visible Spectroscopy-UV-Vis», The canadian journal of chemical engineering,Vol 96 ,2018 ,p.2513.
- [34]:S. K. Tripathi et al,«Irradiation effects on the optical properties of a-Ge-Se-Ag thin films», Journal of Optoelectronics and Advanced Materials Vol 7, 2005, p. 2095 – 2101.
- [35]:E. Şilik,« Electrochromic properties of TiO₂ thin films grown by thermionic vacuum arc method», Thin Solid Films Vol 640,2017 ,p.27–32.
- [36]:A.Yahia ,«Optimization of indium oxide thin films properties prepared by sol-gel spin coating process for optoelectronic applications» ,Thesis doctorat, Unive-rsity Med Khider (Biskra),2019.
- [37]:M. Carter et al ,« Guide to Research Techniques in Neuroscience», published by Elsevier Inc,2015,p. 117-145.
- [38]:University of Cambridge, 15 juin 2021.
- [39]:E. Muchuweni et al , «Synthesis and characterization of zinc oxide thin films for optoelectronic applications», Heliyon Vol 3 (4) , 2017,p.11.

References Chapitre II

- [1]:M. J. Gázquez et al ,« A Review of the Production Cycle of Titanium Dioxide Pigment», Materials Sciences and Applications Vol 5 , 2014, p.441.
- [2]:Z. Youssef,«Nanoparticules de TiO₂ Couplées à Des Photosensibilisateurs Pour Des Applications En Photocatalyse Et En Thérapie Photodynamique»,doctorat thesis,l'Université de Lorraine(France) ,2017.
- [3]:Y. Lan et al,« Mini review on photocatalysis of titanium dioxide nanoparticles and their solar applications», Nano energy Vol 2, 2013,p.1032.
- [4]:I. Ali et al, «Recent advances in syntheses, properties and applications of TiO₂ nanostructures », The Royal Society of Chemistry Vol 8 , 2018, p.30126.

- [5]:A. Fujishima et al,«TiO₂ photocatalysis and related surface phenomena»,Surface Science Reports Vol 63, 2008,p.519-520.
- [6]:F . De Angelis et al,«Theoretical Studies on Anatase and Less Common TiO₂ Phases: Bulk, Surfaces, and Nanomaterials»,Chemical Reviews,American Chemical Society Vol 114,2014, p.9708-9753.
- [7]: D.Ulrike et al , «The surface science of titanium dioxide» , Surface science Vol 48, 2003, P.67.
- [8]:Y.F. zhang et al, «A theoretical study on the electronic structures of TiO₂: Effect of Hartree-Fock exchange», The Journal of Physical chemistry Vol 109(41),2005,p.19271.
- [9]:O.Benkhetta , «Effet de la concentration de la solution sur les propriétés des couches minces de dioxyde de titane déposées par spray pyrolyse ultrasonique», Mémoire de master , Université Med Khider(Biskra),2019.
- [10]:K. Jha. Prafulla et al , «Titanium Dioxide: Applications, Synthesis and Toxicity», published by Nova Science, 2013,p.60,61.
- [11]:A.S.Matuk, «Titania-silica sol-gel coatings on glass»,doctorat thesis,Rutgers University(New Jersey),2018.
- [12]:N. Rahimi et al ,«Review of functional titanium oxides. I: TiO₂ and its modify-cations », Progress in Solid State Chemistry Vol 44(3),2016,p.86-105.
- [13]:J.Low et al ,« Rutile : Properties, Synthesis and Applications», Publishers by Nova Science.Inc, 2012,p.209-228.
- [14]:R. Dongre et al ,« Assorted Dimensional Reconfigurable Materials», published by IntechOpen,2020, Chapter3 p 1-16.
- [15]:A.S Bakri et al , «Effect of Annealing Temperature of Titanium Dioxide Thin Films on Structural and Electrical Properties», International Conference on Engineering, Science and Nanotechnology 2016 ,p.2.
- [16]:R.Messemche ,« Elaboration and characterization of undoped and doped titanium dioxide thin layers by sol gel (spin coating) for photocatalytic applications », doctoratthesis,University Mohamed Khider (Biskra),2021.
- [17]:W.Yan, « Structural and Magnetic Properties of Cobalt Doped Titanium Dioxide »,doctorat thesis, The Chinese University of Hong Kong, 2008.
- [18]:D. d'Elia,« Elaboration and study of TiO₂ nanostructures for hydrogen generation via photolysis of water»,doctorat thesis, École Nationale Supérieure des Mines de Paris, 2011.
- [19]:X. Chen et al,«Titanium Dioxide Nanomaterials: Synthesis, Properties, Modifications, and Applications», Chemical Reviews Vol 107, 2007, p.2915.

- [20]:K.Nakata et al,«Photoenergy conversion with TiO₂ photocatalysis» ,New materials and recent applications,Electrochimica Acta Vol 84, 2012 ,p.104-105.
- [21]:A. Fujishima et al, «Titanium dioxide photocatalysis», Journal of Photochemistry and Photobiology C: Photochemistry Reviews Vol 1 , 2000 ,p.15.
- [22]:X. Zhang et al , «TiO₂ Nanowire Free-Standing Membrane for Concurrent Filtration and Photocatalytic Oxidation Water Treatment, web publication» , published by American Chemical Society , 2010,p. 219-237.
- [23]:T.T. Nguyen et al , «Transparent photovoltaic cells and self-powered photodetectors by TiO₂/ NiO heterojunction» , Journal of Power Sources Vol 481 ,2021 ,p.2 .
- [24]:A.Naldoni et al ,«Photocatalysis with Reduced TiO₂: From Black TiO₂ to Cocatalyst-Free Hydrogen Production»,*ACS Catalysis* Vol 9(1),2019,p.345-364.
- [26]:G. Liu et al , «Cation-Assisted Formation of Porous TiO_{2-x} Nanoboxes with High Grain Boundaries Density as Efficient Electrocatalysts for LithiumOxygen Batteries», ACS CatalysisocatalystFree Hydrogen Production , American Chemical SocietyVol 9 ,2019 ,p.345.
- [25]:G. Liu et al , «Cation-Assisted Formation of Porous TiO_{2-x} Nanoboxes with High Grain Boundaries Density as Efficient Electrocatalysts for LithiumOxygen Batteries», ACS Catalysis Vol 8(3) ,2018,p.1.
- [26]:K. Nakata et al ,«TiO₂ photocatalysis: Design and applications,Journal of Photochemistry and Photobiology C», Photochemistry Reviews Vol 13 ,2012 ,p.170.

References chapter III

- [1] : N.Djehaiche , «Effect of Niobium doping on the properties of Titanium Dioxide (TiO₂) Thin films elaborated by sol-gel(Spin-coating)», memory of master ,Mohamed Khider University (Biskra),2019.
- [2] :M. Reza et al , «Effect of mixed solvent on structural, morphological,and optoelectrical properties of spin-coated TiO₂ thin films, Ceramics Internationa Vol 138 ,2012 ,p. 5843–5851.
- [3] :M. Jung, Perovskite precursor solution chemistry: From fundamentals to photovoltaic applications, Chemical Society Reviews Vol 48(7) , 2019,p.8-9.
- [4] :Y.Lorraine , «Développement par procédé plasma de couches minces de type TiO₂ dopé à l'azote pour la production d'hydrogène par photo-électrolyse de l'eau sous lumière solaire»,these doctorat,Université de Montpellier,Liban, 2018.

- [5]:K. Deva Arun Kumar et al ,« Effect of different solvents on the key structural, optical and electronic properties of sol–gel dip coated AZO nanostructured thin films for optoelectronic applications», J Mater Sci: Mater Electron Vol 29 , 2018, p.887–897.
- [6]:M. Dahnoun et al ,«High Transparent Titanium Dioxide-Anatase Thin Films Deposited by Spin Coating Technique:Effect of Annealing Temperature»,J.of Nanoelectronics and Optoelectronics Vol 13, 2018, p.1-7.
- [7]:R. Messemeche et al,«Elaboration and characterization of nano-crystalline layers of transparent titanium dioxide (anatase-TiO₂) deposited by a sol-gel(spin coating)process»,Surfaces and Interfaces Vol 19, 2020, p.1-6.
- [8]:O. Wiranwetchayan et al,«Effect of alcohol solvents on TiO₂ films prepared by sol-gel method»,Surface & Coatings Ty (2017), p.5echnolog
- [9]:M .Ben Karoui,et al , Optical properties of nanostructured TiO₂ thin films, Journal of Physics: Conference Series Vol 596, 2015, p.2-3
- [10]:W.Yu-chan et al,«Effects of alcohol solvents on anatase TiO₂ nanocrystals prepared by microwave-assisted solvothermal method»,J.Nanopart Res Vol 15,2013,p.1-11.
- [11] A.Sobhe Matuk ,«Titania-silica sol gel coating on glass Coatings On »,doctorat thesis,Rutgers University(New Jersey),2018.
- [12]:Y.Akaltun et al ,The relationship between refractive index-energy gap and the film thickness effect on the characteristic parameters of CdSe thin films,Optics Communications Vol 284 ,2011,p.2307–2311.
- [13]:S. Amirtharajan et al , Electricalinvestigation of TiO₂ thin films coated on glass and silicon substrates-effect of UV and visible light illumination,Applied Nanoscience Vol 6 , 2016 , p.591–598 .
- [14]:M.I.Khan et al,«Structural, electrical and optical properties of multilayer TiO₂ thin films deposited by sol-gel spin coating», Results in Physics Vol 7,2017,p.1437-1439.
- [15]:T.H. Gilani and Dian Rabchuk, «Electrical resistivity of gold thin film as a function of film thickness »,Can. J. Phys. Vol 96,2018,p.272–274.
- [16]:A. K. M. Muaz et al , « Effect of annealing temperatures on the morphology, optical and electrical properties of TiO₂ thin films synthesized by the sol– gel method and deposited on Al/TiO₂/SiO₂/p-Si», Microsyst Technol Vol 22(4), 2016, p.871-881.

Abstract

The effect of solvents on the properties of thin films of (TiO₂) deposited by sol gel (spin-coating).

Transparent semiconducting thin films of titanium dioxide (TiO₂) were deposited on glass substrates by the sol–gel method and spin-coating technique. using methanol, ethanol, isopropanol ,methoxyethanol and ethylene glycol as solvents ,titanium tetraisopropoxide as a precursor and acetyl acetone as a stabilizer agent .The effect of solvent medium on the structural, morphological , optical and electrical properties of TiO₂ thin films were investigated using X-ray diffraction (XRD), scanning electron microscopy (SEM), UV-Vis spectroscopy (UV-Vis) ,Energy-dispersive X-ray spectroscopy (EDS) and Four points method .

The XRD patterns reveals that the films are crystalline with an anatase crystal structure and a preferred grain orientation in the (101) direction and the grains size change between (29.541 nm and 21.197 nm),The morphological properties were investigated by SEM, The surface morphology of the films was found to be strongly dependent on the solvent ,The UV-Visible spectrum indicated that the films are highly transparent in the visible region and their transparency is slightly influenced by the film thickness, with an average value above 80 %, and a shift in optical band gap energy of the films from 3.75 to 3.54 eV for direct allowed ,and from 3.47 to 3.34 eV for indirect allowed, as a function of the solvents , has been observed , In addition, the electrical measures showed that the films have conductivity between (0.0073-66.66) Ω⁻¹ .cm⁻¹.

Key words : Solvents effect, TiO₂ thin films , Sol Gel (sping-coating), structural properties, optical properties .

Résumé:

L'effet des solvants sur les propriétés des couches minces de (TiO₂) déposés par sol gel (spin-coating).

Des couches minces semi-conductrices transparentes de dioxyde de titane (TiO₂) ont été déposées sur des substrats de verre par la méthode sol-gel et la technique de revêtement par centrifugation. utilisant du méthanol, de l'éthanol, de l'isopropanol, du méthoxyéthanol et de l'éthylène glycol comme solvants, du tétraisopropoxyde de titane comme précurseur et de l'acétylacétone comme agent stabilisant. L'effet du milieu solvant sur les propriétés structurales, morphologiques, optiques et électriques des films minces de TiO₂ a été étudié en utilisant la diffraction des rayons X (XRD), la microscopie électronique à balayage (MEB), la spectroscopie (UV-Vis), dispersive en énergie Spectroscopie aux rayons X (EDS) et méthode des quatre points.

Les motifs XRD révèlent que les films sont cristallins avec une structure cristalline anatase et une orientation de grain préférée dans la direction (101) et que la taille des grains change entre (29,541 nm et 21,197 nm), Les propriétés morphologiques ont été étudiées par SEM, La morphologie de surface des films s'est avéré fortement dépendant du solvant, le spectre UV-Visible a indiqué que les films sont très transparents dans la région visible et que leur transparence est légèrement influencée par l'épaisseur du film, avec une valeur moyenne supérieure à 80 %, et un un décalage de l'énergie de la bande interdite optique des films de 3,75 à 3,54 eV pour le direct autorisé, et de 3,47 à 3,34 eV pour le indirect autorisé, en fonction des solvants, a été observé. De plus, les mesures électriques ont montré que les films ont conductivité entre (0.0073-66.66) Ω⁻¹ .cm⁻¹.

Mots clés : Effet solvants, couches minces de TiO₂ , Sol Gel (sping-coating), propriétés structurales, propriétés optiques .

تأثير المذيبات على خواص الأغشية الرقيقة لثاني أكسيد التيتانيوم المترسبة بواسطة سائل هلام (طلاء بالدوران).

تم ترسيب طبقات رقيقة من أنصاف النواقل من ثاني أكسيد التيتانيوم على ركائز زجاجية بطريقة سائل-هلام وتقنية الطلاء الدوراني. باستخدام الميثانول والإيثانول والأيزوبروبانول والميتوكسي إيثانول والإيثيلين جلايكول كمذيبات ورابع إيزوبروبوكسيد للتيتانيوم كسلائف وأسيثيل أسيتون كعامل استقرار. تمت دراسة تأثير وسيط المذيب على الخواص البنيوية والمورفولوجية والضوئية والكهربائية للأغشية الرقيقة من ثاني أكسيد التيتانيوم باستخدام حيود الأشعة السينية، (XRD) والمجهر الإلكتروني الماسح، (SEM) والتحليل الطيفي للأشعة المرئية وفوق البنفسجية (UV-Vis)، مطيافية الأشعة السينية المشتتة للطاقة (EDS) وطريقة الاسابر الأربعة .

تكشف أنماط انعراج الأشعة السينية أن الأغشية متبلورة مع بنية بلورية أاناتاز واتجاه حبيبي مفضل في الاتجاه (101) وأن حجم الحبيبات يتغير بين (29.541 نانومتر و 21.197 نانومتر) ، تظهر صور المجهر الإلكتروني الماسح أن التشكل السطحي للأغشية يعتمد بشدة على المذيب ، وأشار الطيف المرئي للأشعة فوق البنفسجية إلى أن الأفلام شفافة للغاية في المنطقة المرئية وأن شفافيتها تتأثر قليلاً بسماكة الفيلم ، بمتوسط قيمة أكبر من 80٪، ولوحظ تحول في طاقة فجوة النطاق الممنوع للأغشية من 3.75 إلى 3.54 فولت للانتقال المباشر، ومن 3.47 إلى 3.34 فولت للانتقال الغير المباشر ، اعتماداً على المذيبات. بالإضافة إلى ذلك، أظهرت القياسات الكهربائية أن الأفلام لها موصلية بين (0.0073-66.66) اوم⁻¹. سم⁻¹.

الكلمات المفتاحية : تأثير المذيب ، أغشية الرقيقة من ثاني أكسيد التيتانيوم، سائل- هلام (طلاء دوران)، الخصائص البنيوية، الخصائص الضوئية.

